Progenitor stars of type IIn supernovae using the NCR method

Master's thesis
University of Turku
Astronomy
2024
Supervisor:
Dr. Tuomas Kangas
Examiners:
Dr. Tuomas Kangas
Prof. Seppo Mattila

The originality of this thesis has been checked in accordance with the University of Turku quality assurance system using Turnitin Originality Check service.

UNIVERSITY OF TURKU
Department of Physics and Astronomy

Välitalo, Milla Progenitor stars of type IIn supernovae using the NCR method

Master's thesis, 53 pp. 5 pages of appendix
Astronomy
December 2024

Supernovae are massive stars exploding at the end of their lifetime, when the processes active during their life can no longer maintain a stable star. There are multiple ways for a star to become a supernova, and thus they are classified through their distinct types of spectra. They are classified into two main types based on hydrogen, type I without it and type II SNe including hydrogen.

Type IIn supernovae have been classified into their own subtype since the 1990s. They can be recognized from their narrow Hα emission lines, resulting in fairly similar spectra. The narrow Hα line comes from the interaction between the supernova's ejecta and the surrounding material. The progenitor stars of some supernova types are known, but it is still not fully known what kind of composition of star types forms the progenitors of type IIn supernovae and in which quantity.

One way to study the progenitors of type IIn supernovae is to use the normalized cumulative ranking (NCR) method. The method is used to calculate a value based on the supernova's position and the strength of the Hα emission at that location. The NCR value is calculated for both the type IIn supernovae as well as for different types of stars. Since star formation and Hα emission areas correlate, it is possible to estimate the ages and mass of the progenitors.

This study found multiple different stars to be possible progenitors of type IIn supernovae based on their NCR distribution. Especially interesting is how well correlated yellow supergiants and type IIn supernovae are, although yellow supergiants did not exhibit the same multimodality as type IIn supernovae. The best combination of two progenitors was found to be made of red supergiants and late type WN stars or stars of similar mass.

Keywords: supernovae, type IIn, progenitors, normalized cumulative ranking method

Contents

Introduction

In this Master's thesis I study progenitor stars of 74 type IIn supernovae (SNe) using the normalized cumulative ranking (NCR) method. I use Hα images of Large Magellanic Cloud (LMC) and Messier 33 (M33) to calculate NCR values for different types of stars and compare them to the type IIn SNe. Distances of the SNe are simulated for the images to take into account the effects of different distances. The main goal of this thesis is to find what kind of mass distribution of stars fits best the mass distribution of type IIn SNe using the NCR method to learn more about progenitors.

In the first part I explain the method and present the star catalogues and how the stars are arranged into different subsamples. The SN sample and its division into three subsamples are introduced. In the second part I explain how the images are made to simulate different distances. Additionally, in this part the NCR values for the stars are calculated as well as tests done for the different star and SN samples.

In the third part results of the tests are presented. Different combinations of star types are attempted to match the NCR distribution of type IIn SNe with different IIn SNe samples. In the fourth part the results are discussed as well as possible shortcomings with the NCR method. The last part contains conclusions.

1 Theory

1.1 Supernova classification

SNe are classified into two main types, type I and type II SNe. Type I SNe are further divided into type Ia, Ib and Ic SNe. Type I SNe don't have H in their spectra. The subtypes are classified by presence or absence of other lines: type Ia have Si II lines, type Ib He I lines and Ic have no He I and weak or no Si II lines. Type Ia SNe come from white dwarfs (WD), while type Ib and Ic are from core-collapse (CC) progenitors. [1]

Type II SNe have H in their spectra, and they are divided into type II-P, II-L and IIn SNe. Type II-P has a plateau in their light curve, while the light curves of II-L decline linearly on the magnitude scale. Type IIn SNe have narrow emission lines of H in the spectra. [1]

Type Ia SNe originate from WDs that explode as a thermonuclear SN. In single-degenerate (SD) scenario the WD has a companion star, for example a red giant. The WD accretes material from the companion star, until Chandrasekhar mass is reached and it explodes. In double-degenerate (DD) scenario two WDs merge together or collide eachother. [2]

All other SNe with massive progenitors explode as a CC SN. CC SNe start from a minimum mass of 7 to 12 Solar masses when the star collapses under gravity due to lack of internal support [6]. First the fusion inside the star continues until it reaches Fe since the fusion no longer produces energy, and depending on the circumstances the Fe core reaches the the Chandrasekhar limit of 1.2 to 2 Solar masses [3].

After this the core collapses and the density of the core increases, creating a proto-neutron star (NS). A shock wave is created when the outer layers of the star continue to collapse to the core, but they bounce from the proto-NS. As the outer layers continue to collapse, the neutrinos from the proto-NS emit energy enough

to eject the material and create the explosion, even though most of the neutrinos escape into space.[4]

1.1.1 Type IIn supernovae

Type IIn SNe were first introduced in 1990 by Schlegel [5]. Examples of type IIn SN spectra can be seen in Figure 1 taken from ref. [1]. In the Figure all the SNe have a prominent narrow Hα line, which defines this SN type. H lines can have also intermediate or broad components [1], for example SN 1998S [6] and SN 2019zrk [7].

Type IIn SNe have fairly similar spectra. The narrow Hα line is created when the SN's ejecta interacts with material around the SN. The material around the SN could have been from the progenitor's outbursts and winds slightly before it's explosion. [1].

Type IIn-P SNe were introduced by Mauerhan *et al.* [8] as a subtype of IIn SNe. Type IIn-P SNe have defined light curves with plateaus similar to II-P and low masses of ^{56}Ni. IIn-P SNe might come from 8-10 Solar mass electron capture stars or massive stars starting from about 25 Solar masses. Examples of IIn-P SNe are SN 2011ht, SN 1994W and 2009kn. [8]

Circumstellar material (CSM) can be caused by dense and dusty winds from massive stars like red supergiants (RSGs) and yellow hypergiants (YHGs). Another way for a star to have CSM are massive ejections of material from the star, for example in some cases luminous blue variables (LBVs) can have nebulae that are 10 to 20 Solar masses, for example η Carinae with ejection of around 10 to 15 solar masses [9]. Massive stars can also have multiple eruptions of different sizes. [10]

There is evidence that some IIn SNe progenitors could be high mass luminous blue variables (LBVs). For example SN2005gl by Gal-Yam *et al.* (2007) [11], SN2005gj by Trundle *et al.* (2008) [12] and SN2010jl by Smith *et al.* (2011) [13]. Some IIn SNe progenitors could also be RSGs [6].

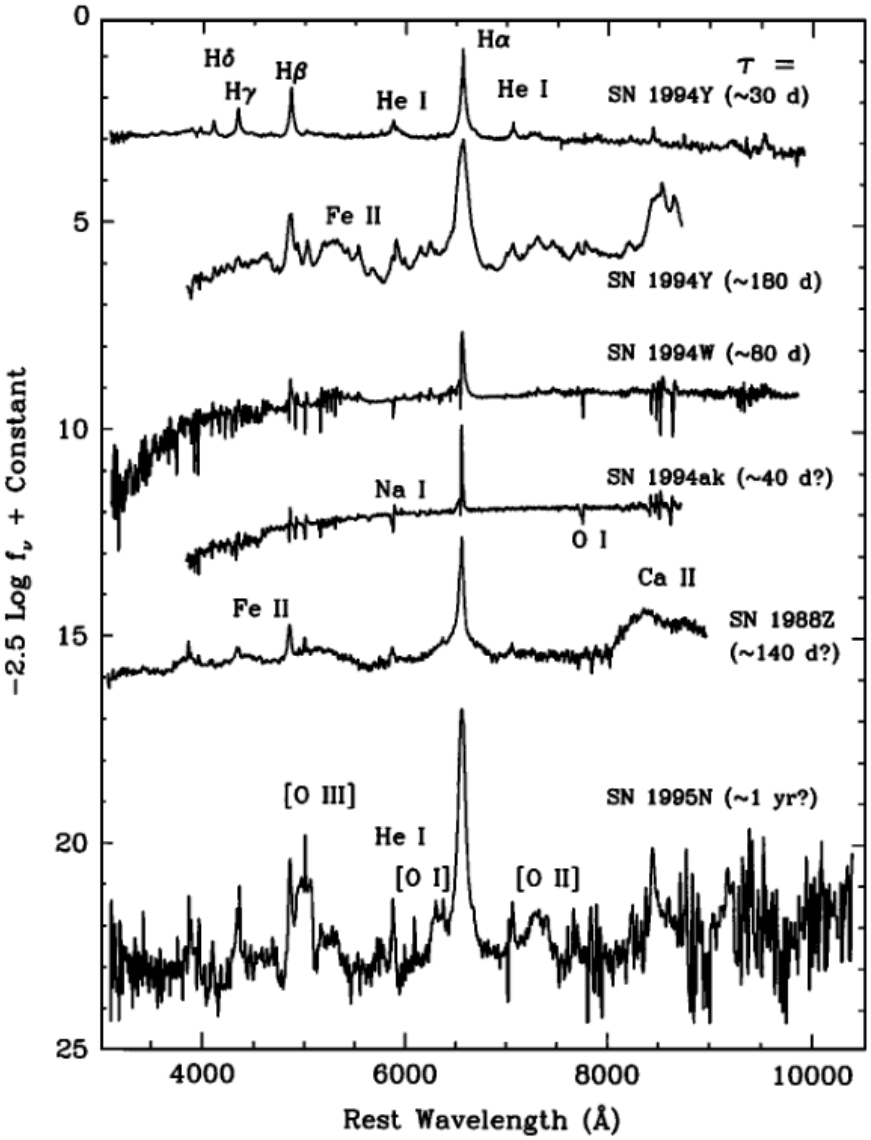

Figure 1. Spectra of six different type IIn supernovae. On the x-axis is the rest wavelength in Ångströms and on the y-axis is the flux. Taken from [1]

.

1.2 Types of evolved stars

RSGs are cold giant stars with effective temperature of about 3500 to 4500 Kelvins and radius of 100 to 1000 Solar radius. Their mass ranges from ∼8 to 40 Solar masses and they have significant mass-loss during their lifetime. [14] RSGs are stars that have left the main sequence. They are on the coldest end of the HR-diagram.

Yellow supergiants (YSGs) are giant stars with effective temperature of 4800 to 7500 Kelvins with initial masses ranging from ∼ 9 to 40 Solar masses. YSGs are a transition phase between the RSG phase and the main sequence or a bluer evolved state with timeframe that is in order of magnitude of 10^4 years. [15]

Wolf-Rayet (WR) stars are massive stars with high mass-loss rates and strong, fast winds. They are divided into two main groups by stages, first are WN stars, which may later become WC stars if they are sufficiently massive. WN stars have He and N in their spectra and WC stars have He, C and O. [16] They are on the hottest end of the HR-diagram.

WN stars are further divided into WN early, WN early H, WN late and WN late H stars. WN early stars are types between WN2-WN5 and WN late types are from WN6 and higher. WN early H and WN late H are divided in the same way except they contain H. WC stars are also divided into WC early and WC late stars, from WC2-WC5 and WC6 and higher, respectively. [17]

LBVs are high luminosity massive stars that vary both photometrically and spectroscopically. They experience instabilitites that result in eruptive mass-loss in different timescales. Mechanisms that cause LBVs' variations are still being studied. [18] Like RSGs, LBVs have also left the main sequence.

1.3 The NCR method

The NCR method was first introduced by Anderson and James (2006) [19] for supernovae and by Fruchter *et al.* (2006) [20] for γ-ray bursts and SNe environments.

The purpose is to find how different kinds of CC supernovae correlate with Hα emission in their host galaxies, since Hα line emission traces star formation. Originally they called the method normalised cumulative rank pixel value function (NCRPVF). The function has values from 0 to 1, with 0 correlating with the least amount of Hα emission, usually in the background pixels. The brightest pixels with the highest amount of Hα emission have value of 1, usually in the center of the galaxy. Hα line emission traces star formation, which correlates with the progenitors of CC supernovae. Longer lived less massive progenitors have time to leave the star forming regions, hence they tend to explode in lower Hα line emission areas and thus lower NCR regions. Sometimes after the shorter lived stars have exploded, the Hα line emission of the area becomes weaker. More massive progenitors tend to explode in the star forming regions or close to them due to their short lifetime, leading into high Hα line emission and higher NCR values. [19]

The NCR value of a pixel is the fraction of Hα emission that is found in pixels with weaker Hα emission. It can be calculated with

$$\mathrm{NCR}_n = \sum_{i=1}^{n} P_i / \sum_{j=1}^{m} P_j, \qquad \text{when} \sum_{i=1}^{n} P_i > 0$$

$$\mathrm{NCR}_n = 0, \qquad \text{when} \sum_{i=1}^{n} P_i \leq 0,$$

where NCR_n is the NCR value of the pixel, P_i is the Hα flux in the pixel, the total number of Hα flux is the sum over P_j from 1 to m, n is rank of the pixel and m is the amount of all the image's pixels. Pixels that have NCR value less than 0 are assigned value 0. [21]

Anderson and James (2008) used a sample of 12 IIn supernovae, with mean NCR value 0.256 $\pm$0.088. Examples for other types are 0.460 $\pm$0.162 for SN IIb, 0.263 $\pm$0.048 for SN IIP and 0.447 $\pm$0.057 for SN Ic. Their findings suggest that IIn supernovae often come from lower progenitor masses than other CC supernovae,

even though they can have some massive progenitors too (see section 1.1.1). [22]

Another study was made by Anderson *et al.* (2012). They had a sample of 19 IIn SNe with mean NCR value 0.213 ± 0.065. The study came to same conclusion about IIn supernovae mostly not having massive progenitors as Anderson and James (2008) [22]. [23]

In a paper by Kangas *et al.* (2017) [17], the authors introduced a new method to use different star catalogues of evolved stars in nearby galaxies and compare them to supernovae. Galaxies used in the paper were LMC and M33. NCR values were calculated for different star types at three simulated distances, 20 Mpc, 35 Mpc and 75 Mpc. An example of a possible IIn progenitor distribution was given as 70 % RSGs and 30 % LBVs with mean NCR value 0.258 ± 0.026. [17]

A larger number of type IIn supernovae were used in a paper by Ransome *et al.* (2022) to find out progenitors of IIn supernovae. They included 77 IIn supernovae in the study. An example of a IIn progenitor distribution was given as 60 % LBVs and 40 % that cannot be connected to Hα emission [24].

1.4 Star catalogues

Older catalogues for M33's RSGs and YSGs were used for subsamples of stars. More recent catalogues for M33's RSGs and YSGs were used for the whole sample. The reason why in some cases different catalogues were used for the full sample and subsamples is that older catalogues had better classification by luminosity. Catalogues were checked in Kangas *et al.* (2017) [17] to ensure good coverage of the entire galaxy.

The catalogue used for LBVs in both LMC and M33 was by Richardson and Mehner (2018) [18]. For LMC the catalogue contains 27 LBV stars, of which 8 are confirmed and 19 are candidates. The paper by Kangas *et al.* (2017) [21] used both confirmed and candidate LBVs, so in this study also both of them were used. For

M33 the catalogue has 35 LBVs, with 5 confirmed and 30 candidates.

The catalogue by Neugent *et al.* (2012) [25] was used for LMC's RSGs and YSGs. There were 543 RSGs and 109 YSGs. These were divided into subsamples by luminosity following the example from Kangas *et al.* (2017). RSGs were divided into log $\frac{L}{L_\odot}$ >4.6 ('RSG 4.6+'), log $\frac{L}{L_\odot}$ <4.6 ('RSG 4.6-') and log $\frac{L}{L_\odot}$ >4.8 ('RSG 4.8+'), and YSGs into log $\frac{L}{L_\odot}$ >4.8 ('YSG 4.8+'). The full samples were also used (RSG all, YSG all). In LMC RSGs of 4.6 are around 9 solar masses [26].

M33's RSGs and YSGs were taken from a survey by Massey, Neugent and Smart (2016) [27]. There were 220 RSGs and 86 YSGs. For subsamples of M33's RSGs and YSGs other catalogues were used. RSG subsamples RSG 4.6+, RSG 4.6- and RSG 4.8+ and YSG subsample YSG 4.8+ were from Drout, Massey, and Meynet (2012) [15].

Wolf-Rayet (WR) stars were divided into 4 subsamples for LMC and 6 subsamples for M33 as described in Sect. 1.2. For LMC they were divided into WC stars and three subsamples of WN stars. For M33 they were divided into three subsamples of WN stars and into three subsamples of WC stars.

The catalogue used for LMC's Wolf-Rayet (WR) stars was by Hainich *et al.* (2014) [16]. In the catalog there are 94 WN stars, of which 56 are classified into subsample "WN late" and 38 into subsample "WN early". The catalogue by Neugent and Massey (2011) was used for M33's WRs [28]. It has 139 WN stars, 38 are classified into subsample "WN late" and 81 into subsample "WN early".

1.5 Supernova sample

The sample of type IIn SNe is taken from Ransome et al. (2022) [24] and divided into subsamples in this study. SN 2019el was left out of the sample because it didn't have a known host galaxy. SN 2015da and 2005ip were also left from the full sample. There was no NCR value for these supernovae in Ransome *et al.* (2022). Table 1

contains all the supernovae that were not used in one or more samples.

Table I. Supernovae not included in the samples, their coordinates, redshift, NCR value, classification (Classif.) and samples they aren't included in

Name	Host	z	NCR value	Classif.	Reason	Sample
SN2019el	-	0.0005	0.003	Silver	No host	1,2,3
SN2005ip	NGC 2906	0.00718	-	Gold	No NCR value	1,2,3
SN2015da	NGC 5337	0.0072	-	Gold	No NCR value	1,2,3
SN2015bf	NGC 7653	0.0142	0.657	-	Without classif.	2
SN2010jj	NGC 812	0.0172	0.000	-	Without classif.	2
PS 15cwt	-	0.0135	0.012	-	Without classif.	2
SN2011js	NGC 1103	0.0138	0.000	-	Without classif.	2
SN2006qt	A034002-0434	0.0100	0.000	-	Without classif.	2
SN2005kd	PGC 14370	0.0150	0.000	-	Without classif.	2
SN2007ak	UGC 3293	0.0156	0.000	-	Without classif.	2
SN2013ha	MCG +11-08-25	0.0131	0.808	-	Without classif.	2
SN2016ehw	MCG+12-08-47	0.0120	0.041	-	Without classif.	2
ASASSN-15lf	NGC 4108	0.0084	0.000	-	Without classif.	2
SN2012ab	A122248+0536	0.0180	0.912	-	Without classif.	2
PS15aip	KUG 1319+356	0.0195	0.860	-	Without classif.	2
SN2006M	PGC 47137	0.0150	0.575	-	Without classif.	2
SN1987C	MCG+09-14-47	0.146	0.0142	-	normal II? [29]	2,3
SN1978G	IC 5201	0.0031	0.000	-	normal II? [29]	2,3
SN2006dn	UGC 12188	0.0171	0.434	-	Ib [30]	2,3
SN1994ak	NGC 2782	0.0085	0.000	Gold	IIn-P	3
SN1994W	NGC 4041	0.0040	0.000	Gold	IIn-P	3
SN1995G	NGC 1643	0.0160	0.007	Gold	IIn-P	3
SN1999eb	NGC 664	0.0180	0.750	Gold	IIn-P	3
SN1999el	NGC 6951	0.0047	0.000	Gold	IIn-P	3

Table I. Continued

Name	Host	z	NCR value	Classif.	Reason	Sample
SN2003G	IC 208	0.0120	0.000	Gold	IIn-P	3
SN2006bo	UGC 11578	0.0153	0.000	Silver	IIn-P	3
SN2009kn	MCG -03-21-06	0.0143	0.000	Gold	IIn-P	3
SN2011ht	UGC 5460	0.0036	0.000	Gold	IIn-P	3
SN2008J	MCG -02-07-33	0.0159	0.808	Gold	Ia-CSM [31]	3
SN2008S	NGC 6946	0.0002	0.000	Gold	Electron-capture SN? [32]	3
SN2006gy	NGC 1260	0.0192	0.907	Gold	SLSN-IIn [33]	3
Gaia14ahl	PGC 1681539	0.0170	0.000	Silver	Ia-CSM [34]	3
SN2015bf	NGC 7653	0.0142	0.657	Silver	Type II [35]	3
SN2006gy	NGC 1260	0.0192	0.907	Gold	SLSN-IIn [33]	3
Gaia14ahl	PGC 1681539	0.0170	0.000	Silver	Ia-CSM [34]	3
SN2015bf	NGC 7653	0.0142	0.657	Silver	Type II [35]	3

Ransome *et al.* (2022) divided their sample into gold and silver subsamples according to Ransome *et al.* (2021). Gold classification is given for supernovae that have IIn features over multiple epochs. The ones classified as silver do not appear to have narrow features over multiple epochs. This is possibly due to insufficient spectroscopy performed on the objects. Active galactic nuclei and gap transients are taken into account considering the classifications. They have also made sure that the narrow features are definitely from CSM interaction and not from other known sources by comparing Hα profiles. [36]

The original sample of 77 type IIn SNe were divided into three samples in this study. Sample 1 contains all the gold and silver classified SNe and also the ones without classification. This first sample containing 74 supernovae is closest to the original sample of 77 supernovae. Mean NCR value for sample 1 is 0.314 ± 0.042.

Sample 2 contains only the gold and silver classified SNe. Size of the sample 2 is 59 supernovae. The mean NCR value for sample 2 is 0.330 ± 0.048. Sample 3 is

the sample 1 except 17 SNe. Sample 3 has 17 gold supernovae, 28 silver SNe and 12 SNe without classification. The SNe without classification had no public spectra. Mean NCR value for sample 3 is 0.343 ± 0.048.

There was private communication with E. Kankare about type IIn-P SNe, and due to that ten SNe were left from sample 3. The progenitors of type IIn-P SNe are probably different than other type IIn SNe and probably less massive, resulting in so-called electron capture SNe. These SNe are SN 1994ak, SN 1994W, SN 1995G, SN 1999eb, SN 1999el, SN 2003G, SN 2006bo, SN 2009kn and SN 2011ht. SN 2008S, while not a SN IIn-P, was removed for similar reasons. The other seven SNe left from the third sample are SN 2006dn, SN 1978G, SN 1987C, 2008J, SN 2006gy, Gaia14ahl and SN 2015bf. It wasn't possible to identify them as type IIn SNe.

2 Methods

2.1 Distance simulation

The distance simulation is made using nearby galaxies LMC and M33, where the NCR values of the stars are measured. This is done to be able to compare the stars to the SNe. The distance simulation simulates different distances for the stars, so that the effect of image quality can be taken into account at close, medium and far distances. The distance and quality of the images affects the NCR values.

Observations in Ransome et al. (2022) [24] were made with three telescopes with different pixel sizes. The IO:O instrument was used with the Liverpool Telescope (LT) and the Wide Field Camera with the Isaac Newton Telescope, both at the Observatorio de Roque de las Muchachos, situated at La Palma in the Canary Islands. [24]

Distances for the supernovae were calculated from redshift with Hubble constant H_0=74.04 ±1.04 km/s/Mpc [37]. Starting with the SN with the highest distance, the supernovae were divided into sets every 5 % interval starting from the maximum distance. There were total of 15 sets, and the average value of each set's distances was used to simulate a distance for an image of LMC and M33. Two of the nearest average distances were more than 5 % away from each other, because there weren't as many nearby SNe as there were SNe at higher distances.

The number of SNe in one set ranged from two to eight SNe for sample 1. The nearest two SNe were at distance 6.6 Mpc and the six SNe at the largest distance were at 78.6 Mpc. Median for sample 1 was 65.9 Mpc.

For sample 2 there were one to six SNe for each set and for sample 3 one to seven SNe. For sample 2 the nearest set was at the same distance as sample 1 at 6.6 Mpc, and the largest distance was at 78.4 Mpc. For sample 3 the distances were 6.4 Mpc and 79.7 Mpc. The second sample's median was 59.5 Mpc and the third one's 62.6

Mpc.

Parameters used were the width of the Gaussian function in gauss, the standard deviation of the noise in rdnoise and the seed in mknoise.

Image Reduction and Analysis Facility (IRAF) is a tool made by National Optical Astronomy Observatory (NOAO) to be used for processing astronomical images. IRAF was used to process the images with tasks `imexam`, `gauss`, `blkavg` and `mknoise`. `Gauss` was used to convolve the images, `blkavg` to change the size of the pixels and `mknoise` to add noise to the images. Parameters used were the width of the Gaussian function in `gauss`, the standard deviation of the noise in `rdnoise` and the seed in `mknoise`. `Rdnoise` was used to add the calculated amount of noise and the seed was used to randomize the noise pattern. A pixel size of 0.3 arcsec and a seeing of 1.7 arcsec were based on the LT images used by Ransome et al. (2022) [24]. `Imexam` was used to get radial plot of the image to get the correct seeing. After `gauss` the images were binned with the use of parameters b1 and b2. Binning was done to ensure that the physical size of a pixel matches that in the images of the SNe. `Rdnoise` was calculated with

$$SNR = \frac{S}{(S + N^2)^{1/2}}, \tag{1}$$

where SNR is signal-to-noise ratio, S is signal value and N is noise. S was taken from an appropriate bright blob from the image and N from the sky area. The SNR was estimated from images graciously provided by C. Ransome to be roughly 8 for distances larger than 26 Mpc and for closer distances roughly 21. The SNR was calculated by measuring S from the example images' blobs and N from the background. Then N was calculated for the simulated images by using the SNR from the example images and measuring S from the image's blob.

The noise level had to estimated for three of the closest distances. Using an SNR of roughly 21 made the images too noisy compared to other images, so the noise

levels for the three images were estimated by eye so that the same structures can be seen in each image with different distance.

In Figure 2 are the negative Hα images of LMC and M33. Figure 3 has an example of the distance simulated images at 26 Mpc and 71 Mpc.

2.2 NCR calculations

NCR values for each image's pixels were calculated with the first code I made using Python (Appendix A). The code takes the distance simulated image as an input and then goes through the pixels calculating their sum. The pixel values are arranged into a Panda dataframe and sorted by their value in ascending order. After this the NCR is calculated for each pixel and saved into .csv format.

NCR values for stars were calculated with the second code (Appendix B). It takes a list containing coordinates for one star type as an input. The list of star coodinates is multiplied either by 10 or 100, depending on the number of stars in the list. The multiplied list of stars used for calculations will be referred to as N from now on. If the number was 100 or less, the original list was multiplied with 100. For lists with more than 100 stars the multiplication was by 10. This was done to ensure that the observed distance distribution was replicated well.

A random number is drawn from the number of supernovae for each sample. Each simulated distance has a certain number of supernovae in it. A corresponding number is assigned to every image and its associated pixel NCR list to make sure that the distribution is correct. Once the star's coordinates are changed into the image's coordinates, a gaussian error with sigma = 1 pixel is added to the coordinates. It is then rounded to the closest pixel to add uncertainty of the object being on the pixel next to it since there is uncertainty in the location of the SNe. The NCR value for the star is then taken from a list of coordinates and NCR values by finding the corresponding x and y coordinates. The NCR values are saved into a list. The

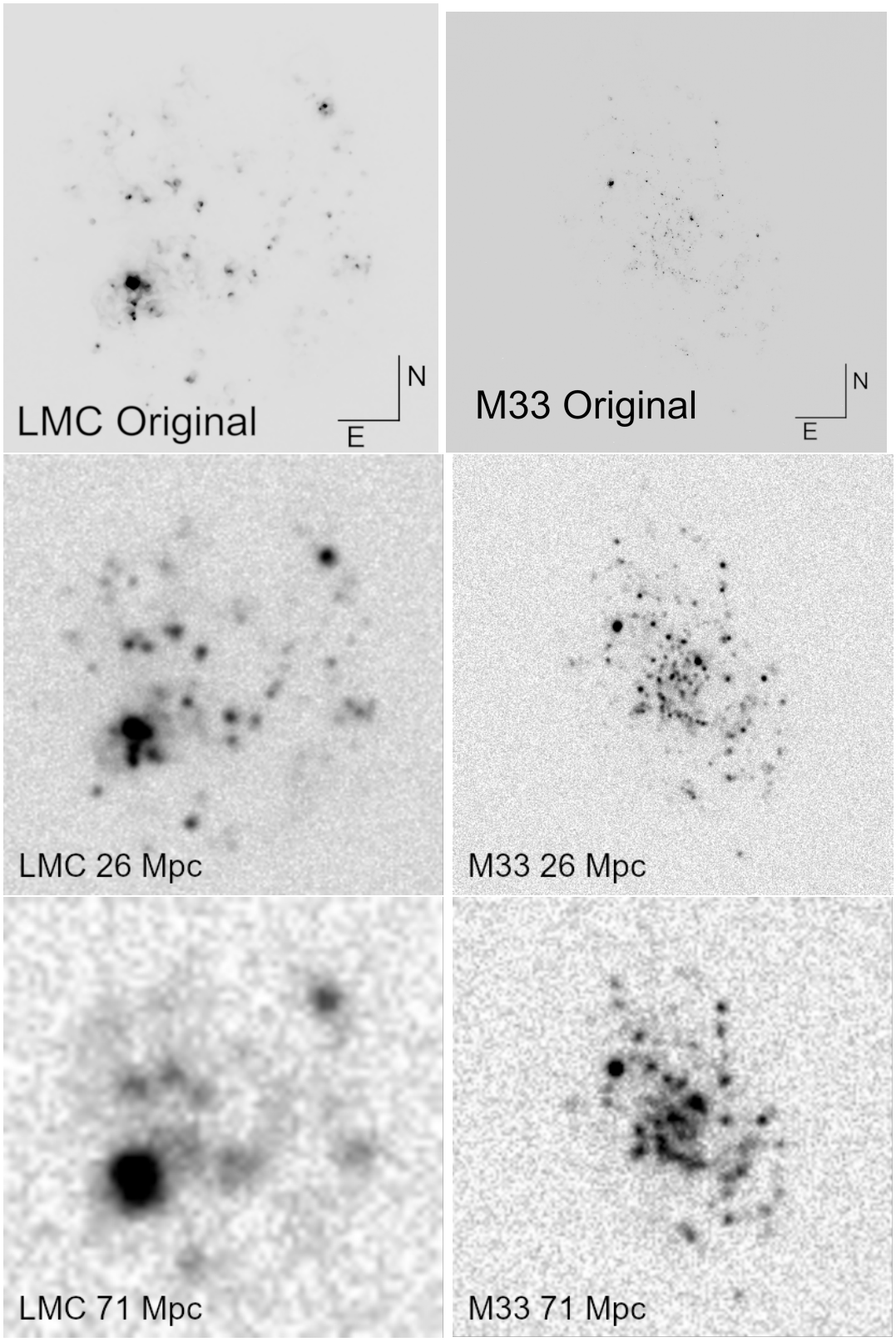

Figure 2. Negative Hα image of LMC taken at Cerro Tololo Inter-American Observatory [38] and M33 taken at Kitt Peak National Observatory [39]. On the left are Hα images of LMC at simulated distances 26 and 71 Mpc and on the right are Hα images of M33 at simulated distances 26 and 71 Mpc. Taken from [38] and [39].

average value and standard deviation for the stars' NCR values are calculated as well.

2.3 Tests

Two tests were used to compare the star NCR distributions against that of the type IIn SNe. The first test used was the Anderson-Darling (AD) test from Python's SciPy, but the highest p-value it reports is 25 %. Another test used was the Kolmogorov-Smirnov (KS) test. Both of the functions have lower limit of 1 %. In the cases where the AD test results reach the limit of 25 %, the results of the KS tests are compared. The tests measure differences between the cumulative distributions by calculating a p-value, which indicates how well they are drawn from the same sample. If the p-value of the test is at least 10 %, then the test sample can not be dismissed as a possible progenitor distribution.

AD and KS tests were calculated with the third code (Appendix C). Both AD and KS tests were from SciPy. The tests needed the NCR list of the stars and supernovae. The lists were sorted by value from smallest to largest and reduced by the amount they were multiplied with before, either 10 or 100, since the sample size affects the tests. The reduction was done by taking every 10th or 100th value from the list and adding them to a new list.

2.4 Progenitor combinations

Progenitor combinations were made to find a distribution of stars that best fit the distribution of type IIn supernovae. They were made with different percentages from two progenitor types, for example RSG 4.6+ - WN late or RSG-LBV that has been used in earlier studies. 60/40 RSG-LBV means that the combination has 60 % RSGs and 40 % LBVs. Combination range between 30/70 and 75/25.

The combinations are made from two possible progenitor types with different masses, to correspond to a potential lower mass progenitor type with small NCR values and a higher mass progenitor type with high NCR values to obtain the shape of the NCR distribution of type IIn SNe.

3 Results

3.1 NCR distributions

3.1.1 LMC

Table II consists of different star types, their mean NCR value and AD and KS tests versus type IIn NCR values using the distance distribution of sample 1 in the LMC. 0.250, the highest AD test value reported by the AD test implemented in SciPy is obtained from comparisons to both the 'RSG 4.8+' and 'YSG all' samples. 'YSG lum4_8+' has an AD test value of 0.105. These three also have the highest KS test values, with 'YSG all' having the highest. All other comparisons resulted in a p-value of less than 10 %. The best 3 matches for each sample are in bold.

Table II. LMC Sample 1: Different star types, their amount, their mean NCR value, standard error of the mean (SEM) for the mean NCR value and AD and KS tests vs type IIn NCR values

Star type	n	$\overline{\text{NCR}}$	SEM(NCR)	AD vs IIn	KS vs IIn
LBV	15	0.436	0.008	0.015	0.046
RSG all	543	0.164	0.003	0.001	0.001
RSG 4.6-	361	0.136	0.004	0.001	0.000
RSG 4.6+	182	0.226	0.006	0.035	0.018
RSG 4.8+	**76**	**0.257**	**0.003**	**0.250**	**0.221**
YSG all	**109**	**0.322**	**0.01**	**0.250**	**0.606**
YSG 4.8+	**37**	**0.363**	**0.005**	**0.105**	**0.329**
WC	24	0.593	0.006	0.001	0.002
WN all	94	0.512	0.004	0.001	0.001
WN early	38	0.376	0.005	0.041	0.135
WN early H	29	0.553	0.007	0.001	0.012
WN late	7	0.801	0.008	0.001	0.005
WN late H	20	0.576	0.008	0.001	0.015

Table III consists of different star types, their mean NCR value and AD and KS test results versus type IIn NCR values using the LMC and sample 2. 'YSG all' and 'YSG 4.8+' have the maximum AD test value of 0.250. Other two over 10 % are 'RSG 4.8+' at AD test value of 0.187 and 'WN early' at 0.196.

The highest KS test values are for the same mentioned star types except for LBV, since it has slightly larger value of 0.124 than 'RSG 4.8+' at 0.12.

Table III. LMC Sample 2: Different star types, their amount, their mean NCR value, SEM and AD and KS tests vs type IIn NCR values

Star type	n	$\overline{\text{NCR}}$	SEM(NCR)	AD vs IIn	KS vs IIn
LBV	15	0.418	0.008	0.031	0.124
RSG all	543	0.150	0.003	0.001	0.001
RSG 4.6-	361	0.125	0.004	0.001	0.000
RSG 4.6+	182	0.206	0.006	0.013	0.01
RSG 4.8+	76	0.241	0.003	0.187	0.12
YSG all	**109**	**0.3**	**0.01**	**0.250**	**0.396**
YSG 4.8+	**37**	**0.331**	**0.005**	**0.250**	**0.677**
WC	24	0.585	0.006	0.001	0.004
WN all	94	0.492	0.004	0.002	0.009
WN early	**38**	**0.353**	**0.005**	**0.196**	**0.566**
WN early H	29	0.533	0.007	0.005	0.045
WN late	7	0.777	0.009	0.001	0.018
WN late H	20	0.558	0.008	0.007	0.065

Table IV consists of different star types, their mean NCR value and AD and KS test results versus type IIn NCR valuesusing the LMC and sample 3. The highest AD test values are again for 'YSG all', 'YSG 4.8+' and 'WN early' at 0.250. Also LBV is over 10 % with value of 0.127.

The highest KS test values are for those four mentioned star types. 'YSG 4.8+' is at 0.586 and 'WN early' at 0.585.

Table IV. LMC Sample 3: Different star types, their amount, their mean NCR value, SEM and AD and KS tests vs type IIn NCR values

Star type	n	$\overline{\text{NCR}}$	SEM(NCR)	AD vs IIn	KS vs IIn
LBV	15	0.402	0.008	0.127	0.335
RSG all	543	0.139	0.003	0.001	0.000
RSG 4.6-	361	0.116	0.004	0.001	0.000
RSG 4.6+	182	0.189	0.006	0.001	0.006
RSG 4.8+	76	0.228	0.003	0.063	0.098
YSG all	**109**	**0.287**	**0.01**	**0.250**	**0.205**
YSG 4.8+	**37**	**0.322**	**0.005**	**0.250**	**0.586**
WC	24	0.567	0.006	0.004	0.016
WN all	94	0.479	0.004	0.019	0.036
WN early	**38**	**0.340**	**0.005**	**0.250**	**0.585**
WN early H	29	0.521	0.007	0.029	0.140
WN late	7	0.778	0.009	0.002	0.022
WN late H	20	0.541	0.008	0.020	0.088

3.1.2 M33

Table V consists of different star types, their mean NCR value and AD and KS test results versus type IIn NCR values using the M33 and sample 1. 'YSG all', 'YSG 4.8+' and LBV have the highest AD test value of 0.250. 'RSG 4.8+' has value of 0.137. The highest KS test value is for 'YSG 4.8+' at 0.557 and LBV at 0.363.

Table V. M33 Sample 1: Different star types, their amount, their mean NCR value, SEM and AD and KS tests vs type IIn NCR values

Star type	n	$\overline{\text{NCR}}$	SEM(NCR)	AD vs IIn	KS vs IIn
LBV	**33**	**0.401**	**0.006**	**0.250**	**0.363**
RSG all	220	0.18	0.006	0.001	0.005
RSG 4.6-	68	0.083	0.002	0.001	0.001
RSG 4.6+	120	0.205	0.008	0.008	0.016
RSG 4.8+	69	0.262	0.003	0.137	0.105
YSG all	**86**	**0.28**	**0.003**	**0.250**	**0.253**
YSG 4.8+	**58**	**0.337**	**0.004**	**0.250**	**0.557**
WC	52	0.499	0.004	0.002	0.002
WC early	28	0.456	0.006	0.068	0.077
WC late	14	0.658	0.007	0.001	0.002
WN all	139	0.483	0.009	0.001	0.000
WN early	81	0.374	0.004	0.068	0.113
WN late	38	0.665	0.005	0.001	0.000

Table VI consists of different star types, their mean NCR value and AD and KS test results versus type IIn NCR values using the M33 and sample 2. The highest AD test values are for LBV, 'YSG lum4_8+', 'WC early' and 'WN early' at 0.25. 'RSG 4.8+' is close with 0.243. LBV has the highest KS test value of 0.866

Table VI. M33 Sample 2: Different star types, their amount, their mean NCR value, SEM and AD and KS tests vs type IIn NCR values

Star type	n	$\overline{\text{NCR}}$	SEM(NCR)	AD vs IIn	KS vs IIn
LBV	**33**	**0.365**	**0.006**	**0.250**	**0.866**
RSG all	220	0.158	0.005	0.001	0.003
RSG 4.6-	68	0.073	0.002	0.001	0.000
RSG 4.6+	120	0.184	0.008	0.243	0.459
RSG 4.8+	69	0.233	0.003	0.055	0.081
YSG all	86	0.251	0.003	0.114	0.191
YSG 4.8+	58	0.130	0.313	0.250	0.45
WC	5200	0.448	0.005	0.074	0.067
WC early	**28**	**0.410**	**0.007**	**0.250**	**0.477**
WC late	14	0.612	0.008	0.006	0.013
WN all	139	0.428	0.01	0.095	0.057
WN early	**81**	**0.343**	**0.004**	**0.250**	**0.653**
WN late	38	0.616	0.006	0.001	0.001

Table VII consists of different star types, their mean NCR value and AD and KS test results versus type IIn NCR values using the M33 and sample 3. Similarly to sample 2, both LBV and 'YSG 4.8+' have AD test value of 0.250.

Table VII. M33 Sample 3: Different star types, their multiplied amount, their mean NCR value, SEM and AD and KS tests vs type IIn NCR values

Star type	n	$\overline{\text{NCR}}$	SEM(NCR)	AD vs IIn	KS vs IIn
LBV	**33**	**0.401**	**0.006**	**0.250**	**0.679**
RSG all	220	0.184	0.006	0.001	0.004
RSG 4.6-	68	0.081	0.002	0.001	0.000
RSG 4.6+	120	0.211	0.008	0.002	0.018
RSG 4.8+	69	0.276	0.004	0.096	0.095
YSG all	86	0.288	0.003	0.169	0.209
YSG 4.8+	**58**	**0.338**	**0.004**	**0.250**	**0.542**
WC	5200	0.499	0.004	0.009	0.014
WC early	28	0.455	0.006	0.231	0.188
WC late	14	0.669	0.006	0.001	0.002
WN all	139	0.484	0.009	0.009	0.007
WN early	**81**	**0.375**	**0.004**	**0.174**	**0.309**
WN late	38	0.668	0.005	0.001	0.000

3.2 Progenitor type combinations

3.2.1 RSG-LBV

Figures are presented to illustrate the comparisons between progenitor types and their combinations against type IIn SNe. In the Figures are shown the cumulative NCR distributions of the combinations of two different progenitors types and type IIn SNe.

Figures 3, 4 and 5 are for combinations of RSG and LBV against all three samples using the LMC. There are five lines for each combination for the five different seeds the code uses for the combinations. The combinations are made by using the multiplied NCR value lists of the stars, by taking random values from those lists until the total number is equal to the number of type IIn SNe in the sample times 100. The results of the tests are the average values of the tests done for each individual combination with different seed. The RSG-LBV combination is made for LMC but not M33, as its catalogue contains both LBVs and LBV candidates.

Table VIII contains the AD and KS-test values for RSG-LBV combinations in LMC against all three samples. The best 3 combinations for each sample are in bold. Unsurprisingly many of the best combinations are very close to each other, for example the combinations that match sample 2 best are 40/60 (AD-test value of 0.23), 45/55 (0.229) and 50/50 (0.218). The best combination for sample 1 is 55/45, 40/60 for sample 2 and 40/60 for sample 3.

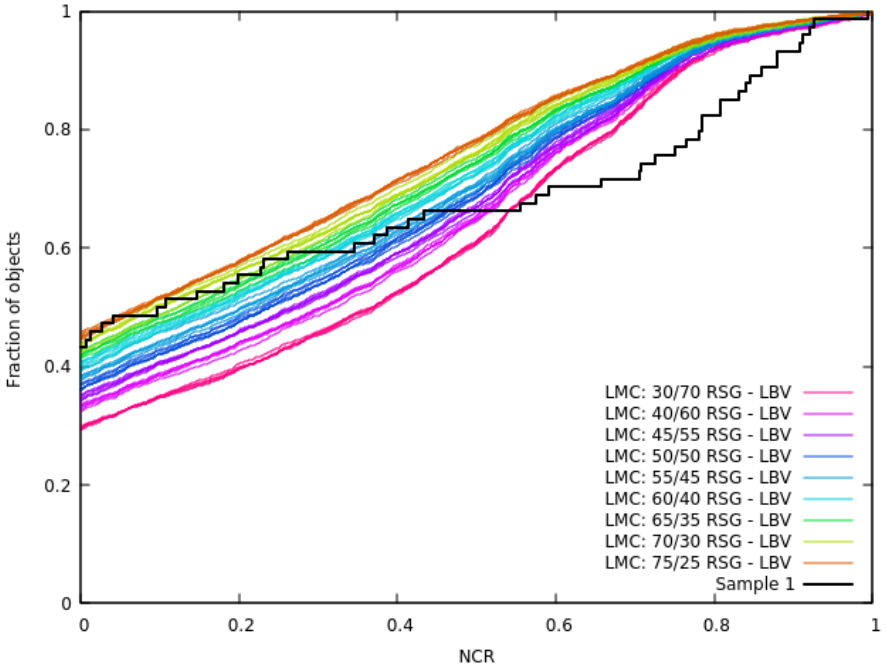

Figure 3. Combination of RSGs and LBVs in the LMC compared to sample 1. On the x-axis is the NCR value and on the y-axis is the fraction of objects.

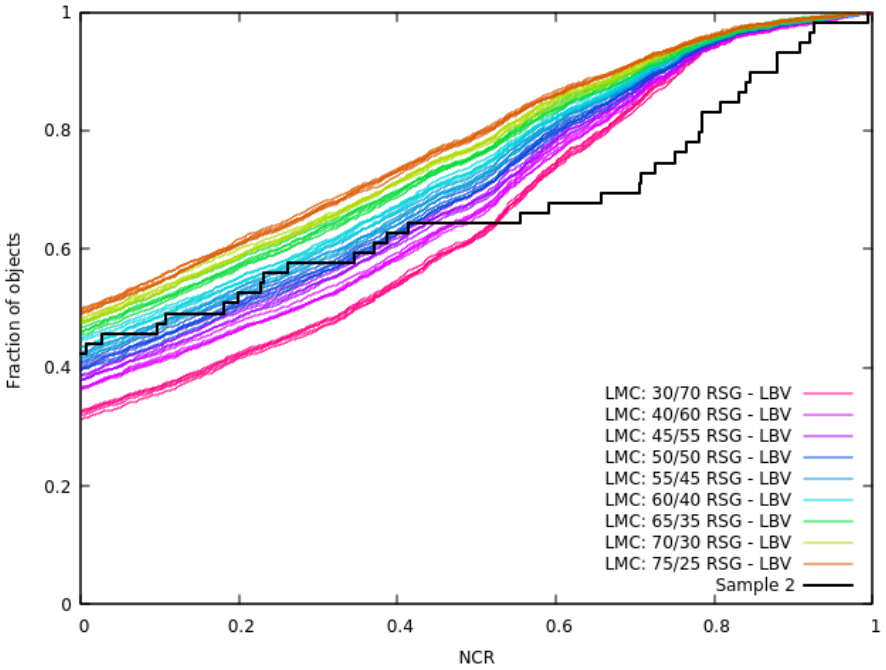

Figure 4. Combination of RSGs and LBVs in the LMC compared to sample 2. On the x-axis is the NCR value and on the y-axis is the fraction of objects.

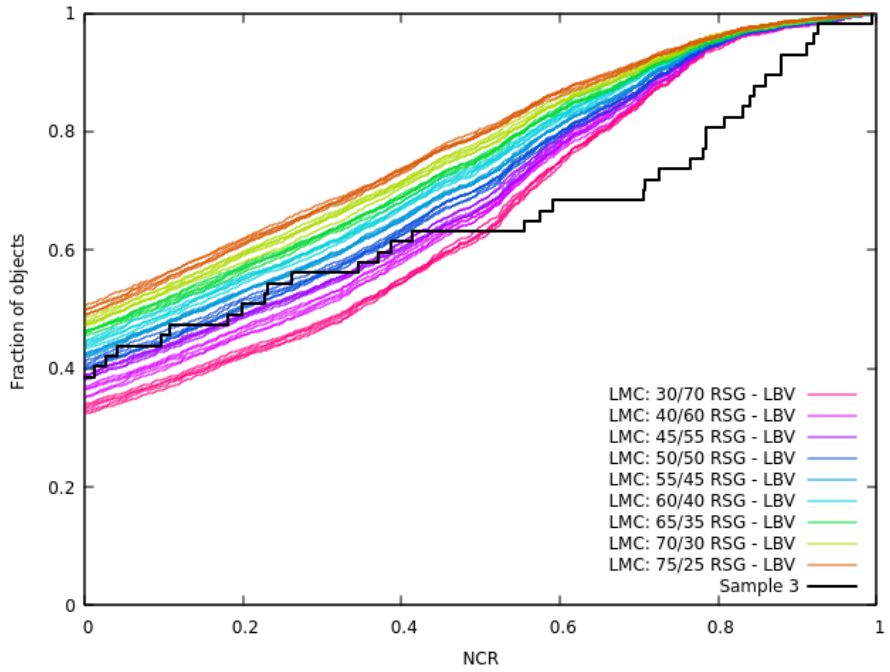

Figure 5. Combination of RSGs and LBVs in the LMC compared to sample 3. On the x-axis is the NCR value and on the y-axis is the fraction of objects.

Table VIII. AD and KS tests for LMC's combinations of RSG-LBV

Combination (/)	AD s1	KS s1	AD s2	KS s2	AD s3	KS s3
30/70	0.0481	0.286	0.147	0.421	**0.193**	**0.24**
40/60	0.108	0.307	**0.23**	**0.346**	**0.201**	**0.24**
45/55	0.142	0.327	**0.229**	**0.28**	**0.197**	**0.24**
50/50	0.165	0.27	**0.218**	**0.242**	0.17	0.192
55/45	**0.204**	**0.27**	0.182	0.175	0.136	0.154
60/40	**0.183**	**0.179**	0.158	0.163	0.091	0.103
65/35	**0.17**	**0.142**	0.111	0.126	0.0646	0.103
70/30	0.147	0.123	0.078	0.114	0.043	0.095
75/25	0.11	0.096	0.054	0.080	0.023	0.064

3.2.2 YSG all and YSG 4.8+

The 'YSG all' and 'YSG 4.8+' samples had high AD and KS test values against type IIn SNe using both the LMC and M33. Figure 6 shows the comparison between 'YSG all' and 'YSG lum 4_8+' in both LMC and M33 against all type IIn samples.

Especially the 'YSG all' sample against samples 2 and 3 in LMC fits the IIn distribution between NCR values of 0 and about 0.4. The same goes for the 'YSG all' sample in M33 against sample 3.

The AD-test value of sample 2 and 3 'YSG all' is at least 0.250 from tables III and III. M33's sample 3 'YSG all' from table VII has 0.169 as AD-test value.

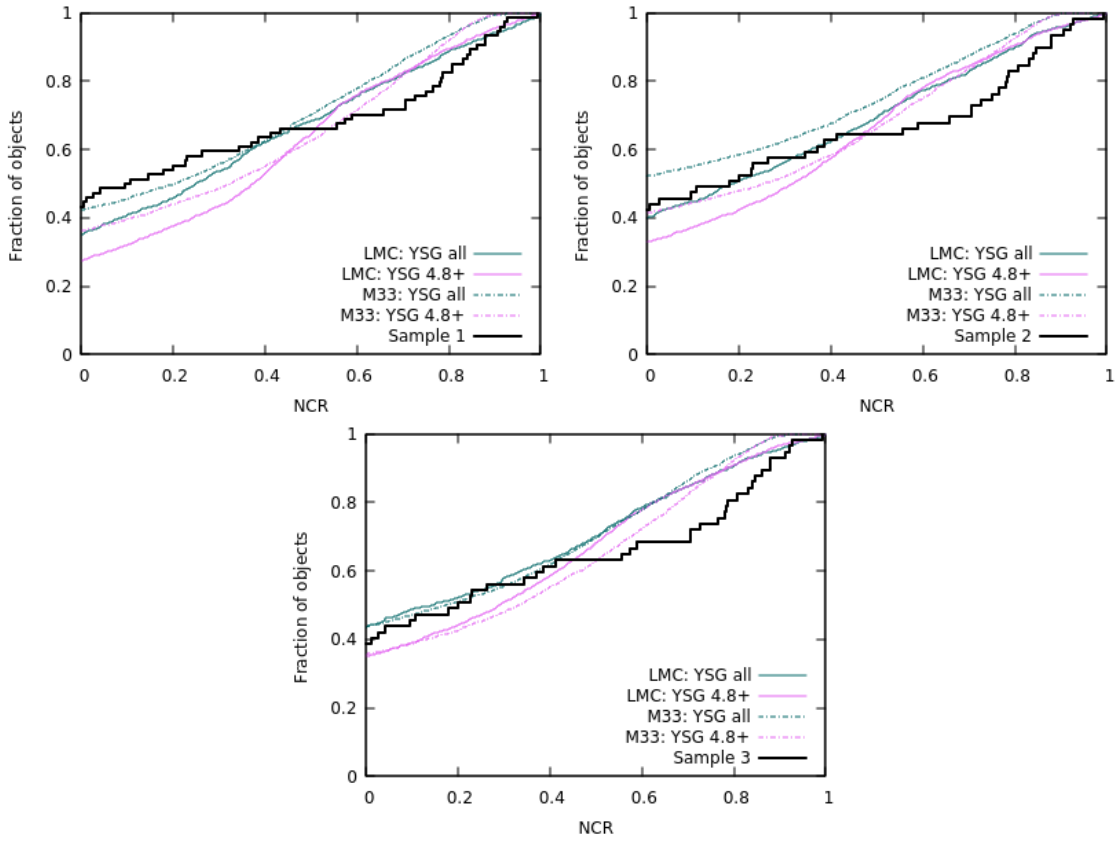

Figure 6. 'YSG all' and 'YSG 4.8+' in the LMC compared to all samples and 'YSG all' and 'YSG 4.8+' in the M33 compared to all samples. On the x-axis is the NCR value and on the y-axis is the fraction of objects.

3.2.3 RSG 4.6+ - WN late

The 'RSG 4.6+ - WN late' combination was attempted since the combination contains types with both low and high mean NCR values. NCR values of LBVs are lower than those of 'WN late' stars, since LBV contains mostly candidates. 'WN late' stars' need at least 40 to 50 Solar masses [40] and that better compares with some observed progenitors of type IIn SNe, RSGs being another possible progenitor types. In Kangas *et al.* In [17] only RSGs in M33 were found to be consistent by AD test with type IIn SNe and in Anderson *et al.* (2012)[23] the mean NCR value 0.213 ± 0.065 of type IIn SNe indicates relatively low-mass progenitors.

Figures 7, 8 and 9 contain combinations of 'RSG 4.6+' and 'WN late' against all the samples in LMC. Table IX contains the results of AD and KS-tests for the combinations. The best 3 combinations for each sample are in bold text. The best combinations for LMC were 75/25 for sample 1, 65/35 for sample 2 and 60/40 for sample 3.

Table IX. AD and KS tests for LMC's combinations of RSG 4.6+ - WN late

Combination (/)	AD s1	KS s1	AD s2	KS s2	AD s3	KS s3
30/70	0.001	0.008	0.005	0.055	0.089	0.240
40/60	0.004	0.04	0.037	0.191	0.250	0.572
45/55	0.011	0.076	0.08	0.302	0.250	0.726
50/50	0.026	0.012	0.185	0.502	0.250	0.928
55/45	0.063	0.221	0.250	0.715	**0.250**	**0.989**
60/40	0.135	0.327	**0.250**	**0.876**	**0.250**	**0.996**
65/35	**0.227**	**0.487**	**0.250**	**0.985**	**0.250**	**0.969**
70/30	**0.250**	**0.648**	**0.250**	**0.900**	0.250	0.788
75/25	**0.250**	**0.830**	0.250	0.685	0.250	0.633

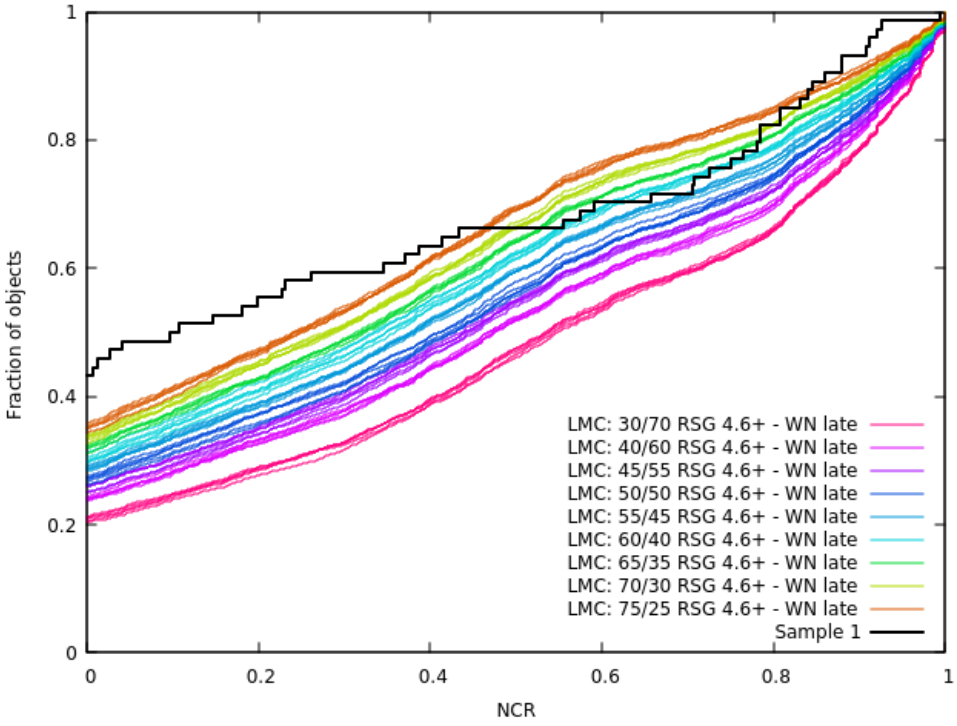

Figure 7. Combination of 'RSG 4.6+' and 'WN late' in the LMC compared to sample 1. On the x-axis is the NCR value and on the y-axis is the fraction of objects.

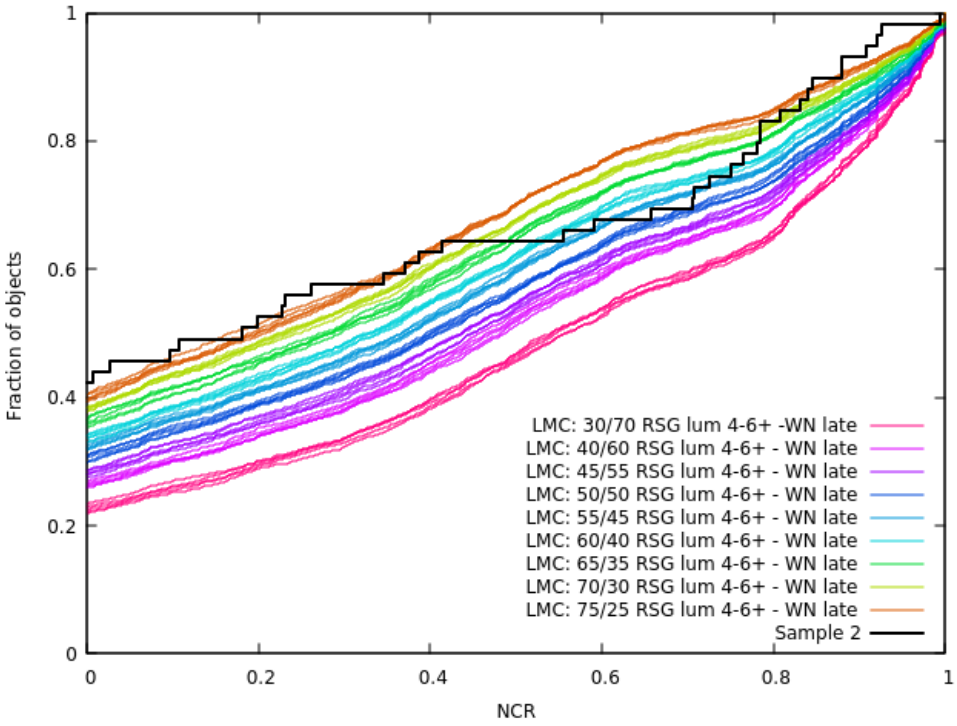

Figure 8. Combination of 'RSG 4.6+' and 'WN late' in the LMC compared to sample 2. On the x-axis is the NCR value and on the y-axis is the fraction of objects.

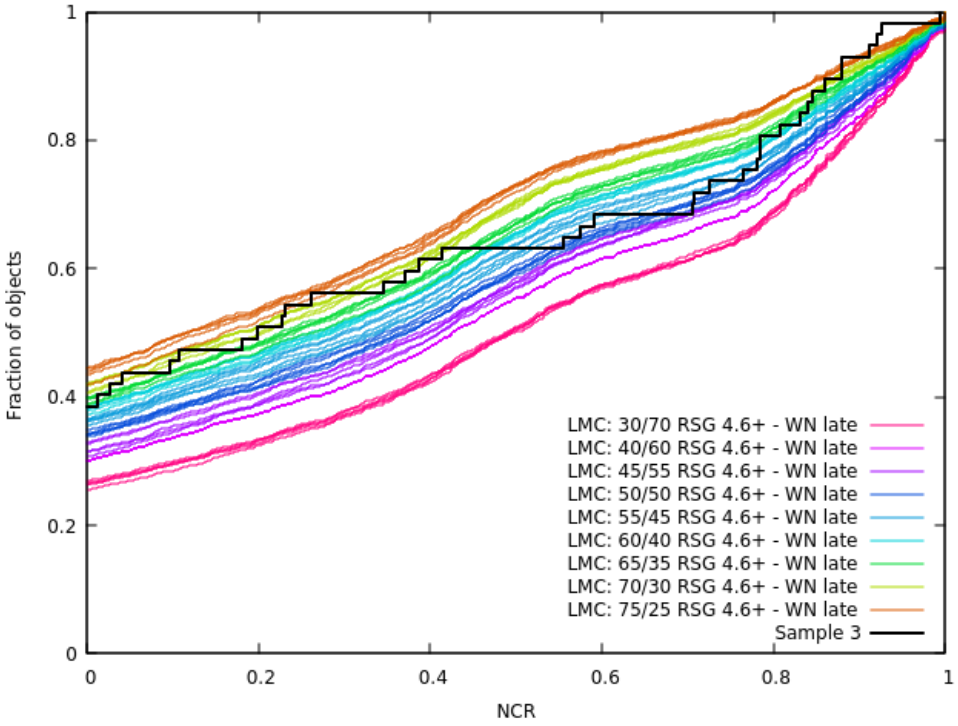

Figure 9. Combination of 'RSG 4.6+' and 'WN late' in the LMC compared to sample 3. On the x-axis is the NCR value and on the y-axis is the fraction of objects.

Figures 10, 11 and 12 contain combinations of 'RSG 4.6+' and 'WN late' against all the samples in M33. Table X has AD and KS test values for all the combinations of 'RSG lum 4_6+' and 'WN late' against the three samples, in bold text are the best 3 combinations. The best combinations for M33 were 70/30 for sample 1, 65/35 for sample 2 and 65/35 for sample 3.

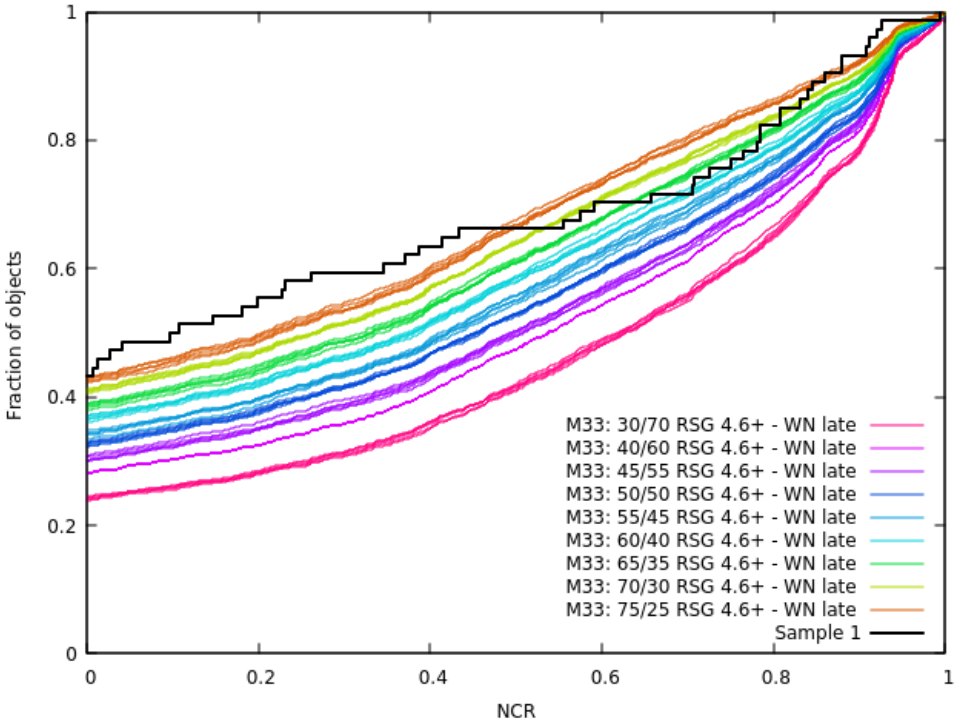

Figure 10. Combination of 'RSG 4.6+' and 'WN late' in the M33 compared to sample 1. On the x-axis is the NCR value and on the y-axis is the fraction of objects.

Table X. AD and KS tests for M33's combinations of 'RSG 4.6+ - WN late'

Combination (/)	AD s1	KS s1	AD s2	KS s2	AD s3	KS s3
30/70	0.001	0.005	0.037	0.089	0.016	0.029
40/60	0.009	0.028	0.245	0.346	0.119	0.149
45/55	0.029	0.069	0.250	0.533	0.220	0.262
50/50	0.087	0.142	0.250	0.685	0.250	0.426
55/45	0.196	0.270	0.250	0.912	0.250	0.633
60/40	0.250	0.463	**0.250**	**0.988**	**0.250**	**0.813**
65/35	**0.250**	**0.702**	**0.250**	**0.991**	**0.250**	**0.982**
70/30	**0.250**	**0.898**	**0.250**	**0.924**	0.250	0.788
75/25	**0.250**	**0.875**	0.250	0.715	**0.250**	**0.813**

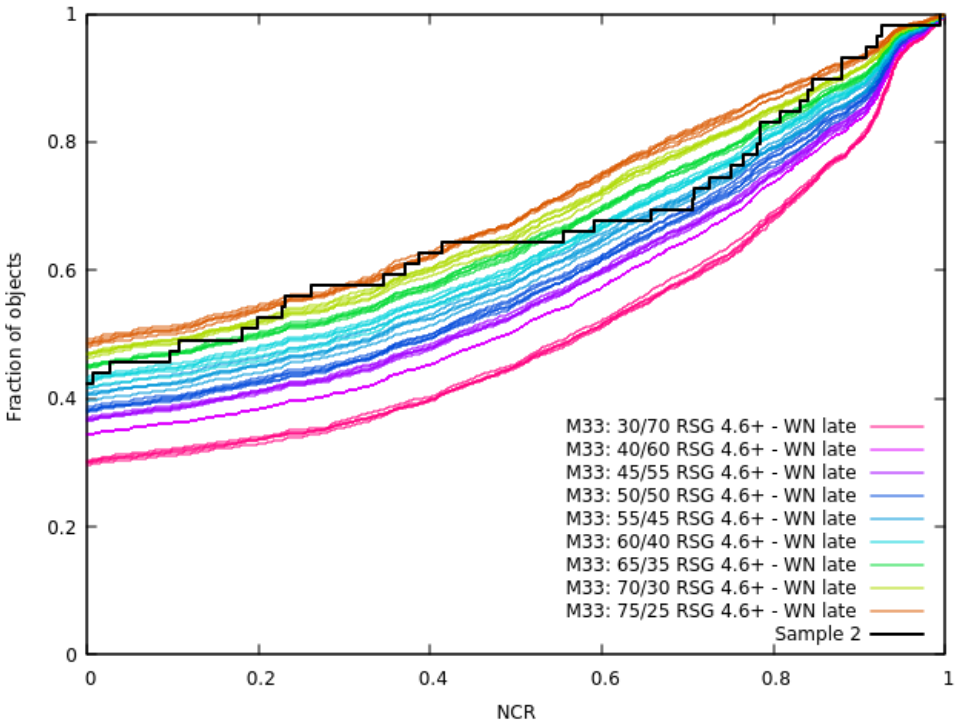

Figure 11. Combination of 'RSG 4.6+' and 'WN late' in the M33 compared to sample 2. On the x-axis is the NCR value and on the y-axis is the fraction of objects.

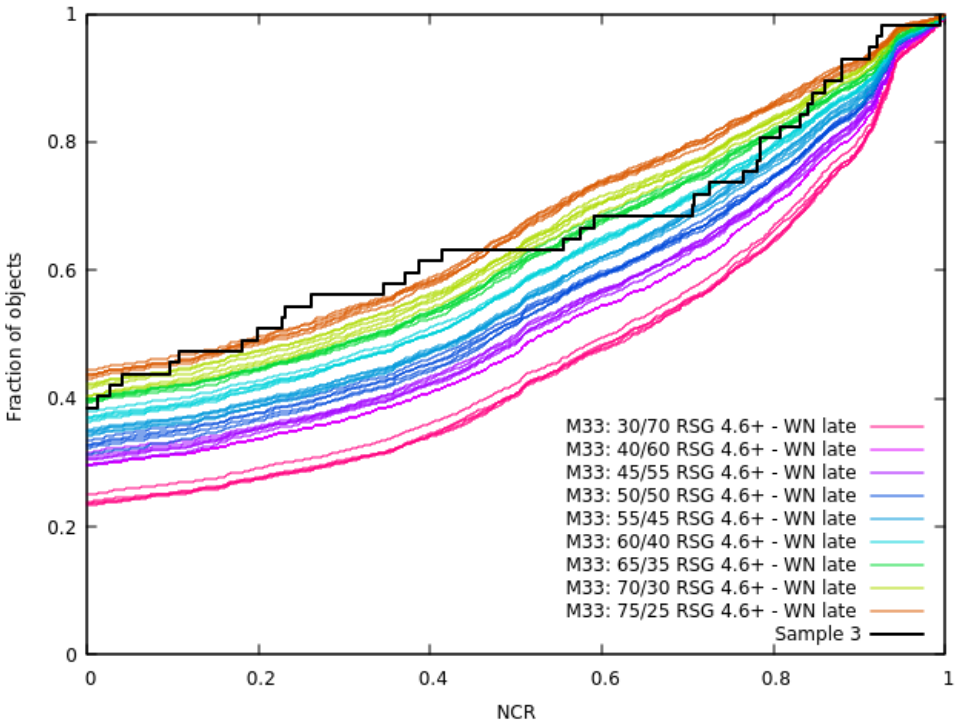

Figure 12. Combination of 'RSG 4.6+' and 'WN late' in the M33 compared to sample 3. On the x-axis is the NCR value and on the y-axis is the fraction of objects.

3.2.4 Identifying NCR distributions that match best with the sample

Histograms were made to have another way to compare the best progenitor types with the type IIn SNe NCR distribution. For histograms the distributions are compared with the fraction of simulated objects instead of a cumulative distribution. The apparent peaks in the distributions can easily be located with intervals of 0.1 NCR value.

Figures 13, 14 and 15 have histograms against all the samples in LMC. They all contain the best individual distribution of YSGs, the best combination of 'RSG 4.6+ - WN late', RSG-LBV and the sample. Since the AD and KS test were made with 5 different seeds, the test that had the result closest to the average of those 5 KS-tests was used in the histogram.

'YSG all' was used in Figure 13 for sample 1, because the 'YSG all' sample was a better match than 'YSG 4.8+'. For the other two samples the AD-tests were better for 'YSG 4.8+' than 'YSG all'. The best 'RSG 4.6+ - WN late' distributions were 75/25 for sample 1, 65/35 for sample 2 and 65/35 for sample 3. The best RSG-LBV distributions were 55/45 for sample 1, 45/55 for sample 2 and 40/60 for sample 3.

Looking at table VIII it should be noted that using RSG-LBV combinations, the LMC and sample 2, the combinations 40/60 and 45/55 are extremely close to each other. 40/60 has AD-test value of 0.23 and 45/55 has 0.229. The same goes for the RSG-LBV combinations 40/60 and 45/55 using sample 3 and the LMC, with values 0.201 and 0.197 for AD-tests and 0.24 and 0.24 for KS-test values.

For sample 1 in Figure 13 the second highest peak for the SNe is between 0.7-0.9. 'YSG all' has a small second peak at 0.3-0.4. 'RSG 4.6+ - WN late' 75/25 has secondary peaks, the first one is wider at 0.3-0.5 and the other one is at 0.9-1.0. The secondary peak for RSG-LBV 55/45 is at 0.5-0.6. The highest peak for all of them is at 0-0.1 because of all the zero NCR values.

Sample 2 in Figure 14 has a slightly more prominent second peak for the SNe at

0.7-0.8. 'YSG 4.8+' has the wider second peak at 0.4-0.6. 'RSG 4.6+ - WN late' 65/35 has the second peak at 0.9-1.0. For RSG-LBV 45/55 the second peak is at 0.5-0.6 in the same way as in sample 1 in Figure 13.

The third sample in Figure 15 has a wider second peak for the SNe at 0.7-0.9. 'YSG 4.8+' has also a wider peak between 0.4-0.6, in the same way as in sample 2 in Figure 14. 'RSG 4.6+ - WN late' 60/40 has its second peak at 0.8-0.9. RSG-LBV 40/60 has the second peak at 0.5-0.6, which is same as in sample 1 in Figure 13 and sample 2 in Figure 14.

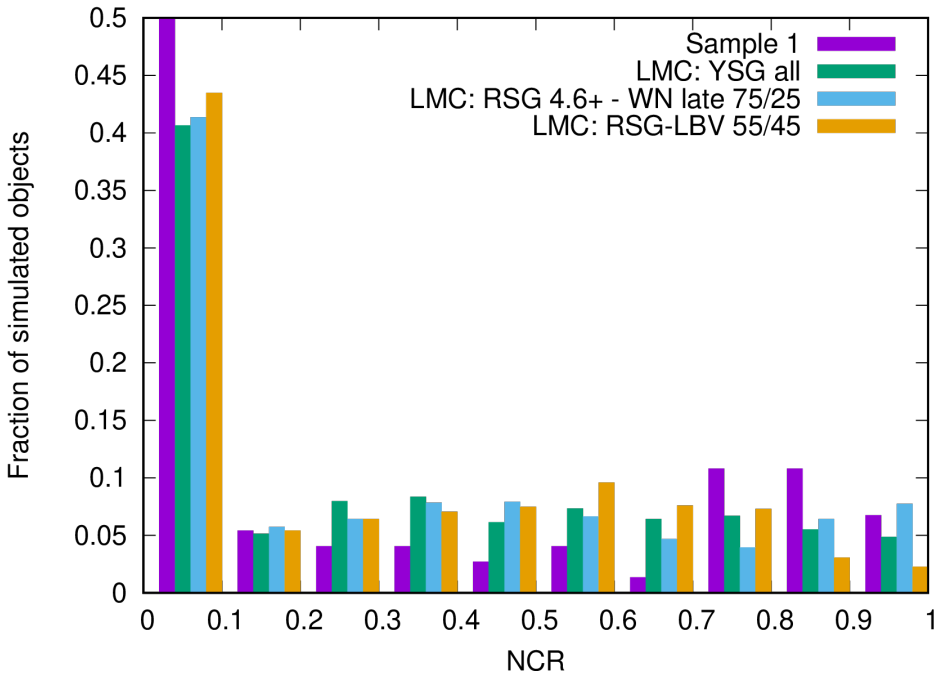

Figure 13. LMC: Sample 1, YSG all, RSG 4.6+ - WN late 75/25 and RSG-LBV 55/45. On the x-axis is the NCR value and on the y-axis is the fraction of simulated objects.

Figures 16, 17 and 18 have histograms against all the samples in M33. They all contain the best individual distribution of YSGs, the best combination of 'RSG 4.6+ - WN late' and the sample. The best individual YSG was 'YSG 4.8+' for all the three samples. The best 'RSG 4.6+ - WN late' distributions were 70/30 for sample 1, 60/40 for sample 2 and 65/35 for sample 3. In a same way as LMC, the highest peak for all the distributions is at 0-0.1.

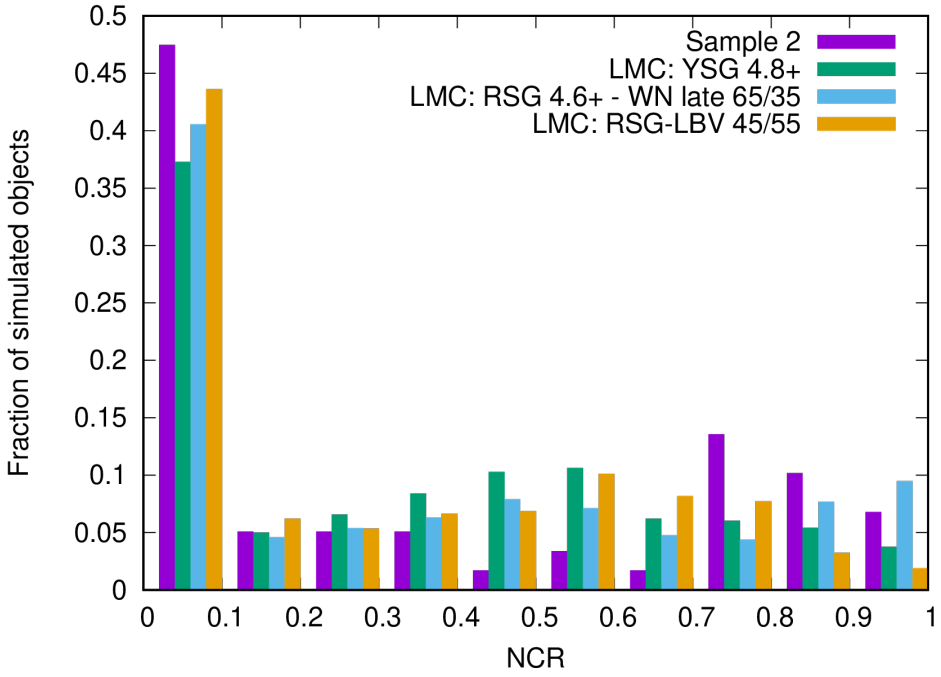

Figure 14. LMC: Sample 2, YSG 4.8+, RSG 4.6+ - WN late 75/25 and RSG-LBV 55/45. On the x-axis is the NCR value and on the y-axis is the fraction of simulated objects.

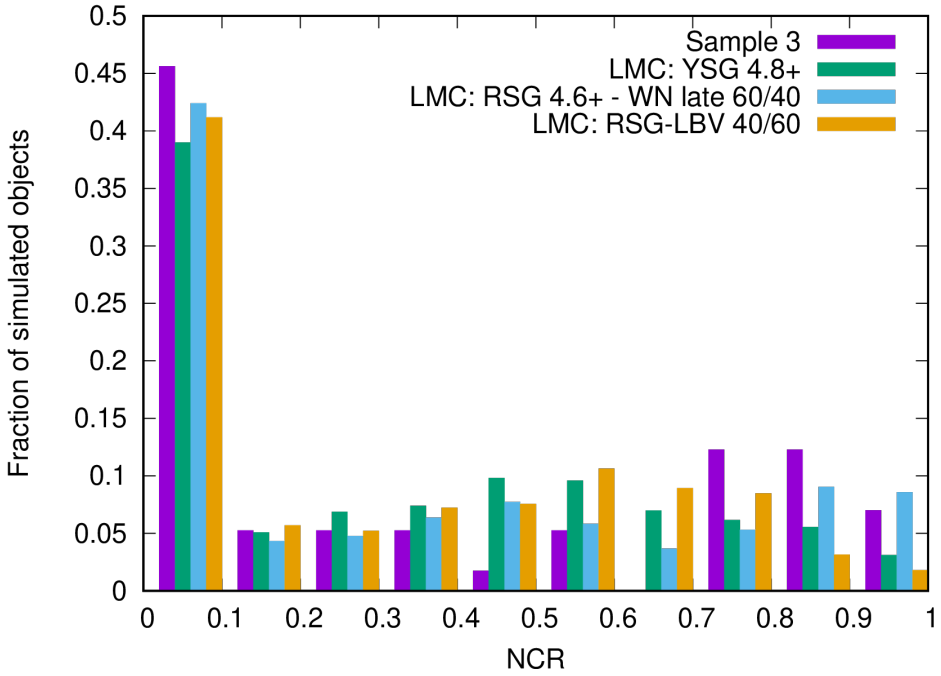

Figure 15. LMC: Sample 3, YSG 4.8+, RSG 4.6+ - WN late 60/40 and RSG-LBV 40/60. On the x-axis is the NCR value and on the y-axis is the fraction of simulated objects.

For sample 1 in Figure 16 the second highest peak for 'YSG 4.8+' is between 0.6-0.8 NCR. Sample 1 SNe have their second peak at 0.7-0.9 NCR. 'RSG 4.6+ - WN late' 70/30 has a second peak at 0.9-1.0 and two similar small peaks at 0.4-0.5 and 0.8-0.9 NCR.

Sample 2 in Figure 17 has a slightly more prominent second peak for the SNe at 0.7-0.8. 'YSG 4.8+' is at fairly similar level between 0.5 and 0.8. 'RSG 4.6+ - WN late' 60/40 has it's second peak at 0.9-1.0.

The third sample in Figure 18 has a bit wider second peak for SNe at 0.7-0.9. 'YSG 4.8+' has its second peak at 0.7-0.8, but in the same way as in sample 2 in Figure 17 'YSG 4.8+' has almost similar level between 0.5-0.8. 'RSG 4.6+ - WN late' 65/35 peaks at 0.9-1.0 in the same way as in with sample 1 and 2, but with 70/30 and 60/40 combination.

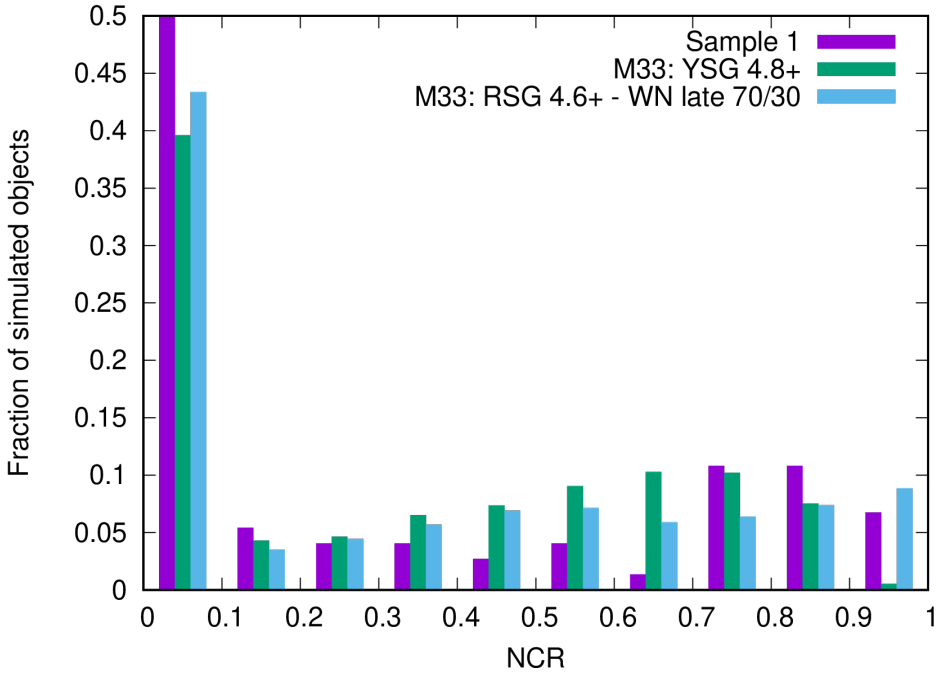

Figure 16. M33: Sample 1, YSG 4.8+ and RSG 4.6+ - WN late 70/30. On the x-axis is the NCR value and on the y-axis is the fraction of simulated objects.

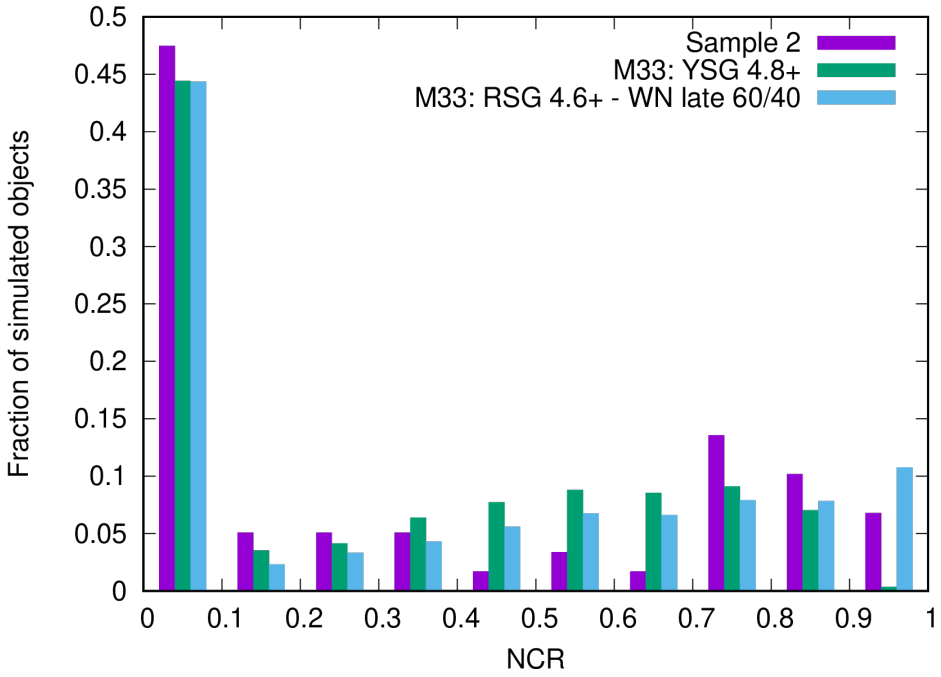

Figure 17. M33: Sample 2, YSG 4.8+ and RSG 4.6+ - WN late 60/40. On the x-axis is the NCR value and on the y-axis is the fraction of simulated objects.

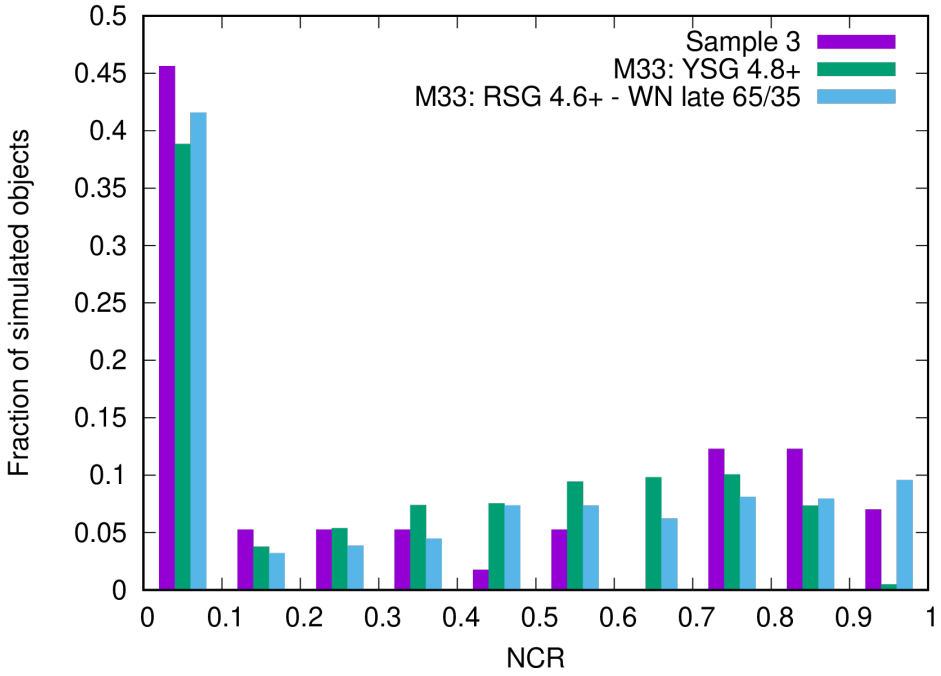

Figure 18. M33: Sample 3, YSG 4.8+ and RSG 4.6+ - WN late 65/35. On the x-axis is the NCR value and on the y-axis is the fraction of simulated objects.

3.2.5 Non-zero NCR values

In their study Ransome *et al.* (2022) [24] made a Figure including non-zero NCR values of the type IIn SNe and comparing them to the diagonal. The diagonal represents an ideal distribution of progenitors that are associated with Hα line emission and thus star formation. They came to a conclusion of a distribution of 60 % LBVs and 40 % of progenitors that cannot be connected to Hα emission.

Comparison between different SNe types with non-zero NCR values was made to test whether the non-zero NCR values from other types of SNe also follow the diagonal, not just only type IIn. Figure 19 has non-zero NCR values of SNe Ib, Ic, Ibc, II and IIn SNe from Anderson *et al.* (2012) [23] and the three samples of type IIn SNe based on Ransome *et al.* (2022) [24].

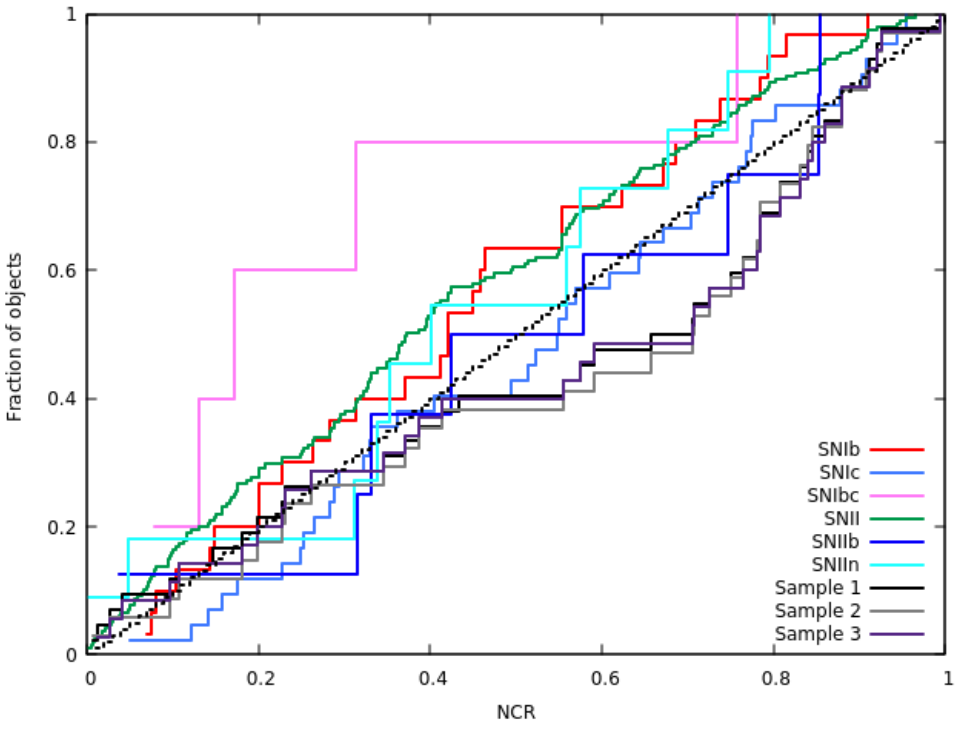

Figure 19. Non-zero NCR values from different types of SNe from Anderson *et al.* (2012) [23] combined with SNe from Anderson and James (2008) [22] and the three samples of type IIn SNe based on Ransome *et al.* (2022) [24]. On the x-axis is the NCR value and on the y-axis is the fraction of objects. Taken from [23], [22] and [24].

Table XI has the number of non-zero SNe (n) for each different type, their mean NCR value, standard error of the mean NCR value and AD and KS tests vs diagonal. All of them except SN Ibc and SN II have AD-test of at least 0.250 vs the diagonal. The best AD-tests were with SN Ic with value of 0.886 and SN IIn with value of 0.691.

Table XI. Non-zero NCR values: Different SN type types, their amount, their mean NCR value, standard error of the mean for the mean NCR value and AD and KS tests vs diagonal

SN type	n	$\overline{\text{NCR}}$	SEM(NCR)	AD vs diagonal	KS vs diagonal
SN Ib	30	0.431	0.045	0.250	0.445
SN Ic	42	0.526	0.040	0.250	0.886
SN Ibc	5	0.290	0.19	0.157	0.149
SN II	195	0.42	0.02	0.021	0.075
SN IIn	11	0.437	0.076	0.250	0.691
Sample 1	42	0.554	0.048	0.250	0.16
Sample 2	34	0.573	0.052	0.250	0.115
Sample 3	35	0.559	0.053	0.250	0.158

Dividing the NCR values into zero and non-zero NCR values doesn't tell too much about the progenitors, since the number of zero NCR values is dependent on the distances of the SNe and the quality of the images.

4 Discussion

In Ransome *et al.* (2022) ([24]) the example for type IIn SNe progenitors was given as a distribution of 60 % LBVs and 40 % of progenitors that cannot be connected to Hα emission. In this study the same SN sample of type IIn SNe was used and three different subsets within this sample were tested to further find more accurate results.

The first sample in this study with 74 SNe is the closest sample to the sample from Ransome *et al.* The second sample in this study has the SNe classified as silver or gold by Ransome *et al.* (2021) [36] and none of the other SNe from Ransome *et al.* (2022), that weren't classified with the silver or gold classification. Gold classification was given for the supernovae that have IIn features over multiple epochs. This sample was meant to consist of well checked type IIn SNe. But as seen from table I, some of them maybe should have been left out, like SN 2008J, SN 2006gy, Gaia14ahl and SN 2015bf.

The third sample in this study has 57 SNe, consisting of all the SN except type IIn-P classified (10 SNe), 6 SNe for which there wasn't enough evidence to be IIn SNe and 1 SN that was SLSN-IIn. All these were listed in table I.

In Figures XII and XIII are summaries of the best 3 progenitor types for each sample. Both 'YSG 4.8+' and 'YSG all' alongside 'WN early' are good fits in LMC. For sample 1 there is also 'RSG 4.8+'. In M33 the best fits for all samples are LBVs. Then there are also 'YSG 4.8+' and 'WN early' for two samples. 'YSG all' is found in sample 1 and 'WC early' in sample 2.

The results could be due to differences between the galaxies and the numbers of stars in star types. The main difference is that LMC has lower metallicity and a younger star population. Also for example LMC has 7, and M33 has 38 WN late stars, before list multiplication.

Table XII. Summary: Best progenitor types for LMC with AD and KS test vs IIn

Sample	Star type(AD vs IIn/ KS vs IIn)		
1	YSG all (0.250/0.606)	RSG 4.8+ (0.250/0.221)	YSG 4.8+ (0.105/0.329)
2	YSG 4.8+ (0.250/0.677)	YSG all (0.250/0.396)	WN early (0.196/0.566)
3	YSG 4.8+ (0.250/0.586)	WN early (0.250/0.585)	YSG all (0.250/0.205)

Table XIII. Summary: Best progenitor types for M33 with AD and KS test vs IIn

Sample	Star type(AD vs IIn/ KS vs IIn)		
1	YSG 4.8+ (0.250/0.557)	LBV (0.250/0.363)	YSG all (0.250/0.253)
2	LBV (0.250/0.866)	WN early (0.250/0.653)	WC early (0.250/0.477)
3	LBV (0.250/0.679)	YSG 4.8+ (0.250/0.542)	WN early (0.174/0.309)

Table XIV. Summary: Best progenitor types for LMC and M33 with AD and KS test vs IIn

Sample	Star type(AD vs IIn/ KS vs IIn) LMC	Star type(AD vs IIn/ KS vs IIn) M33
1	YSG all (0.250/0.606))	YSG 4.8+ (0.250/0.557)
	RSG 4.8+ (0.250/0.221	LBV (0.250/0.363)
	YSG 4.8+ (0.105/0.329)	YSG all (0.250/0.253)
2	YSG 4.8+ (0.250/0.677)	LBV (0.250/0.866)
	YSG all (0.250/0.396)	WN early (0.250/0.653)
	WN early (0.196/0.566)	WC early (0.250/0.477)
3	30/70 (0.193/0.24)	55/45 (0.250/0.989)
	40/60 (0.201/0.24)	60/40 (0.250/0.996)
	45/55 (0.197/0.24)	65/35 (0.250/0.969)

Two combinations of possible progenitors were made in this study, RSG-LBV and 'RSG 4.6+ - WN late'. In Figures XVI and XV are summaries of the best 3 combinations for each sample. In M33 only the 'RSG 4.8+ - WN late' combination was tested, since its LBV catalogue contains predominantly LBV candidates.

Table XV. Summary: Best combinations of RSG-LBV and RSG 4.8+ - WN late for LMC with AD and KS test vs IIn

Sample	RSG-LBV (AD vs IIn/ KS vs IIn)	RSG 4.8+ - WN late (AD vs IIn/ KS vs IIn)
1	55/45 (0.204/0.27)	65/35 (0.227/0.487)
	60/40 (0.183/0.179)	70/30 (0.250/0.648)
	65/35 (0.17/0.142)	75/25 (0.250/0.830)
2	40/60 (0.23/0.346)	60/40 (0.250/0.876)
	45/55 (0.229/0.28)	65/35 (0.250/0.985)
	50/50 (0.218/0.242)	70/30 (0.250/0.900)
3	30/70 (0.193/0.24)	55/45 (0.250/0.989)
	40/60 (0.201/0.24)	60/40 (0.250/0.996)
	45/55 (0.197/0.24)	65/35 (0.250/0.969)

Table XVI. Summary: Best combinations of RSG-LBV and RSG 4.8+ - WN late for M33 with AD and KS test vs IIn

Sample	RSG 4.8+ - WN late (AD vs IIn/ KS vs IIn)
1	65/35 (0.250/0.702)
	70/30 (0.250/0.898)
	75/25 (0.250/0.875)
2	60/40 (0.250/0.988)
	65/35 (0.250/0.991)
	70/30 (0.250/0.924)
3	60/40 (0.250/0.813)
	65/35 (0.250/0.982)
	75/25 (0.250/0.813)

Some of the combination results from AD tests using the LMC are very close to each other, for example RSG-LBV at 40/60 and 45/55 for sample 2. In general the difference between samples is that the percentage of RSGs is higher the lower the sample is, and the higher the sample is the higher is the percentage of LBVs. For 'RSG 4.6+ - WN late' the KS test results are the best for when the majority of the combination is from 'RSG 4.6+'. The single best combination is in sample 3 60/40 with 0.996 KS test value, although 55/45 and 65/35 are very close too.

Between the two combinations 'RSG 4.6+ - WN late' has significantly higher KS tests. In Figure 9 is 'RSG 4.6+ - WN late' for sample 3, where it can be seen that the best fit between the combination and sample 3 is between 0.5-0.8 NCR value. Between 0 and 0.4 'RSG 4.6+ - WN late' doesn't follow the type IIn distribution as well. The RSG-LBV in Figure 5 for sample 3 matches the type IIn distribution well, but on the other hand at 0.4-0.9 the RSG-LBV is a poor fit.

For M33 the fractions of best combinations for 'RSG 4.6+ - WN late' are very similar to those of LMC. For sample 3 there is clearer difference between the best three combinations, as 65/35 has KS test value 0.982 and both 60/40 and 75/25 have 0.813. In Figure 12 around 0.2-0.4 NCR value there is more difference between the distributions and type IIn SNe as in LMC. All the 'RSG - WN late' combinations are consistent with type IIn SNe using sample 3 and the LMC. The same goes for using M33 and sample 3 except for one combination, 30/70.

In the histograms 13, 14, 15, 16, 17, 18 for the three samples there is a high peak at 0-0.1 NCR value for all the samples, types and combinations of possible progenitors. The second peak for the type IIn SNe is at 0.7-0.9 in all the samples.

None of the combinations or progenitor types used in the histograms have peak at the same place for LMC. The 'YSG 4.8+' stars in M33 have a second peak that overlaps with the type IIn SNe at 0.7-0.8 in all three samples. Other than the first peak at 0-0.1 and for the 'YSG 4.8+' stars in M33 there is no clear resemblance

between the combinations and type IIn SNe that can be seen from the histograms.

In Figure 20 is the Hertzsprung-Russell diagram for LMC, where the middle section is for YSGs and the section on the right for RSGs. From around log $\frac{L}{L_\odot}$ 4.8+ the initial mass of a YSG is 15 to 25 solar masses, maybe even 35 solar masses. From log $\frac{L}{L_\odot}$ 4.6- the mass is 12 Solar masses or less. For 'RSG 4.6+' the mass range is 12 to 25 solar masses. [25]

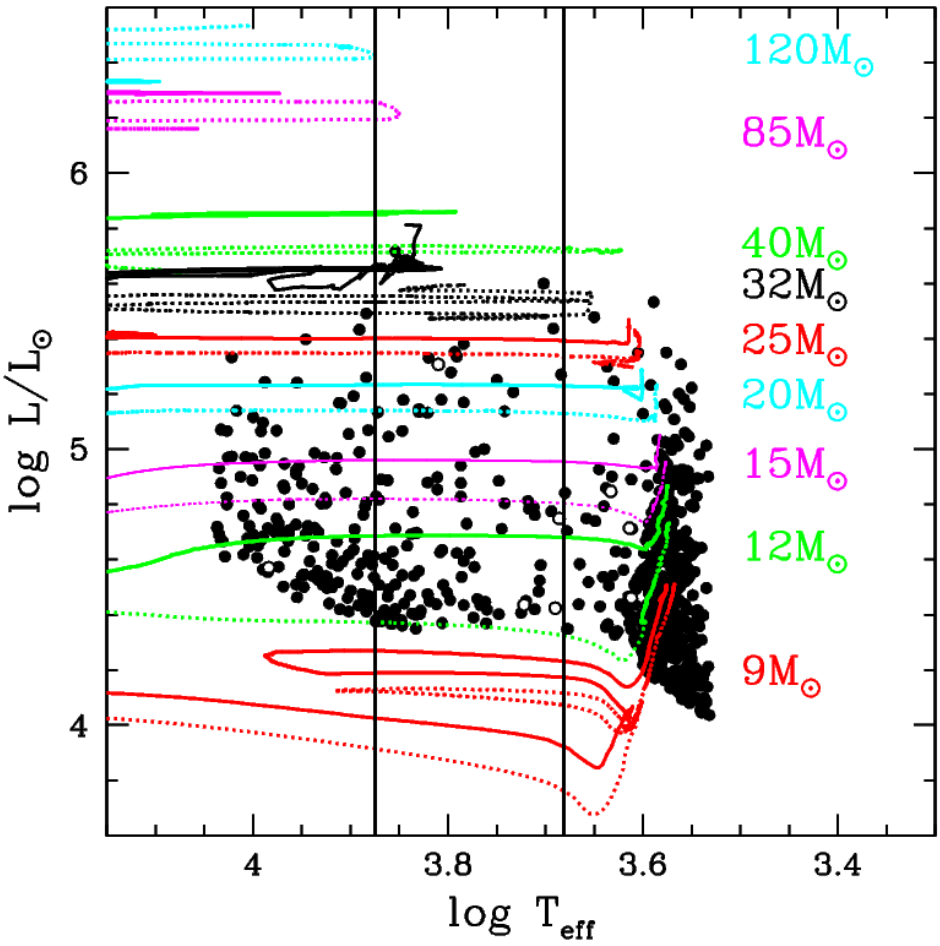

Figure 20. Hertzsprung-Russell diagram for Large Magellanic Cloud, section in the middle is for YSGs and the section on the right is for RSGs. On the x-axis is logarithm of effective temperature of the star and in the y-axis is logarithm of the star's luminosity in Solar luminosity. Taken from [25].

The mean NCR values of the YSGs and 'YSG 4.8+' are very close to the samples of type IIn SNe. For example sample 1 has mean NCR value 0.314 ± 0.042, and it's

'YSG all' has 0.322 ± 0.01 and 'YSG 4.8+' 0.363 ± 0.005 as seen in table II. There problem with YSGs is that the plot in Figure 6 versus type IIn SNe doesn't explain the dip around 0.7 NCR value in distribution of type IIn SNe.

In study by Kangas *et al.* (2017) [17] RSGs were found to be the best match regarding AD-test but not mean NCR value for type IIn SNe using M33, while LBVs had different distribution as well as mean NCR value. On the other hand YSGs were found to match type II-P in LMC, type II-L and IIb in both LMC and M33.

5 Conclusions

The goal of this thesis was to study the progenitors of 74 type IIn SNe with the NCR method. The aim of this study was to find the NCR distribution of stars that best fits the NCR distribution of type IIn SNe and thus find the possible mass range of the progenitors.

This study found that a combination with similar mass or age distribution as YSGs or YSGs with log $\frac{L}{L\odot}$ >4.8 in this study are the best fit as possible progenitors for type IIn SNe. The best combination of two possible progenitor types was found to be combination of RSGs with log $\frac{L}{L\odot}$ >4.6 and late WN stars, with the best-matching combinations being 60/40 % and 65/35 % in the LMC and M33, respectively, for sample 3.

Comparing the results to previous study by Ransome *et al.* (2022) ([24]), this study found the best RSG-LBV distribution to be 40/60 % using the LMC and sample 2 which is similar to the Ransome *et al.* (2022) findings, although the combination of RSGs with log $\frac{L}{L\odot}$ >4.6 and late WN stars appears to be a more likely progenitor mass combination based on the tests added on this study. Other combinations were also consistent and thus cannot be excluded as possibilities. It should be noted that YSGs being less massive than those that have been directly observed to be progenitors of type IIn SNe, there probably needs to be a combination of two or more types of progenitors.

Type IIn-P SNe cannot be differentiated from other IIn SNe within the parameters of this study. In the future it would be useful avenue of improvement to repeat the study larger sample size. There were some oversights in the previous study that were attempted to be rectified in this study, for example removing the zero NCR values and including some non-IIn SNe types.

One of the caveats for this method are the distances to the SNe and the galaxies. Longer distances lower the image quality, increase the number of zero NCR values

and add uncertainty to the NCR values. The number of nearby galaxies that can be observed also limits the method, since good star catalogues are needed to compare the SNe with different star types. Also different galaxy types should be taken into account.

References

[1] A. V. Filippenko, Optical spectra of supernovae, Annual review of astronomy and astrophysics **35**, 309-355 (1997).

[2] M. Livio and P. Mazzali, On the progenitors of Type Ia supernovae, Physics Reports **736**, 1-23 (2018).

[3] L. Rezzolla *et al*, The Physics and Astrophysics of Neutron Stars, Springer, Astrophysics and Space Science Library **457**, (2018).

[4] K. Maeda, Stellar evolution, SN explosion, and nucleosynthesis, Ithaca: Cornell University Library (2022).

[5] E. M. Schlegel, A new subclass of Type II supernovae?, MNRAS **244**, 269-271 (1990).

[6] A. Fassia *et al.*, Optical and infrared spectroscopy of the type IIn SN 1998S: days 3-127, MNRAS **325**, 907-930 (2001).

[7] C. Fransson *et al.*, SN 2019zrk, a bright SN 2009ip analog with a precursor, A&A **666**, A79 (2022).

[8] J. C. Mauerhan *et al.*, SN 2011ht: confirming a class of interacting supernovae with plateau light curves (Type IIn-P) MNRAS **431**, 2599–2611 (2013).

[9] N. Smith, The Dusty Homunculus Nebula of η Carinae, ASP Conference Series **332**, (2005).

[10] S. Nathan, Circumstellar Material Around Evolved Massive Stars, Société Royale des Sciences de Liège, Bulletin **80**, 322-334 (2011).

[11] A. Gal-Yam *et al.*, On the progenitor of sn 2005gl and the nature of type IIn supernovae, ApJ **656**, 372-381 (2007).

[12] C. Trundle *et al.*, SN 2005 gj: evidence for LBV supernovae progenitors?, A&A **483**, L47-L50 (2008).

[13] N. Smith *et al.*, A massive progenitor of the luminous type IIn supernova 2010jl, ApJ **732**, 63 (2011)

[14] E. Levesque, Astrophysics of Red Supergiants, (2017)

[15] M. R. Drout, P. Massey, and G. Meyne, The yellow and red supergiants of M33, ApJ **750**, 97 (2012).

[16] R. Hainich *et al.*, The Wolf-Rayet stars in the Large Magellanic Cloud: A comprehensive analysis of the WN class, A&A **565**, A27 (2014).

[17] T. Kangas *et al.*, Core-collapse supernova progenitor constraints using the spatial distributions of massive stars in local galaxies, A&A **597**, (2017).

[18] N. D. Richardson and A. Mehner, The 2018 Census of Luminous Blue Variables in the Local Group, AAS **2** 121 (2018).

[19] P. A. James and J. P. Anderson, The Hα Galaxy Survey, III. Constraints on supernova progenitors from spatial correlations with Hα emission, A&A **453**, 57-65 (2006).

[20] A. S. Fruchter *et al.*, Long γ-ray bursts and core-collapse supernovae have different environments, A&A **441**, 463–468 (2006).

[21] T. Kangas, Observational studies of core-collapse supernova progenitors and their environments (2017).

[22] J. P. Anderson and P. A. James, Constraints on core-collapse supernova progenitors from correlations with Hα emission, MNRAS **390**, 1527-1538 (2008).

[23] J. P. Anderson *et al.*, Progenitor mass constraints for core-collapse supernovae from correlations with host galaxy star formation, MNRAS **424**, 1372-1391 (2012).

[24] C. L. Ransome *et al.*, An Hα survey of the host environments of 77 type IIn supernovae within $z < 0{,}02$, MNRAS **000**, 1–13 (2022).

[25] K. F. Neugent *et al.*, Yellow and Red Supergiants in the Large Magellanic Cloud, ApJ **749**, 177 (2012).

[26] S. J. Smartt *et al.*, The death of massive stars - I. Observational constraints on the progenitors of Type II-P supernovae, MNRAS **395** 1409-1437 (2009).

[27] P. Massey, K. F. Neugent and B. M. Smart, A Spectroscopic Survey of Massive Stars in M31 and M33, AJ **152**, 62 (2016).

[28] K. F. Neugent and P. Massey, The Wolf-Rayet content of M33, ApJ **733**, 123 (2011).

[29] R. Barbon, The Asiago Supernova Catalogue - 10 years after Astronomy and Astrophysics Supplement **139**, 531-536 (1999).

[30] P. Antilogus *et al.*, Supernova Classifications: Type Ib SN 2006dn and Type Ia SN 2006do, The Astronomer's Telegram **854** (2006).

[31] F. Taddia *et al.*, Supernova 2008J: early time observations of a heavily reddened SN 2002ic-like transient, A&A **545**, L7 (2012).

[32] M. T. Botticella *et al.*, SN 2008S: an electron-capture SN from a super-AGB progenitor?, MNRAS **398** (2009).

[33] N. Smith *et al.*, SN 2006gy: Discovery of the Most Luminous Supernova Ever Recorded, Powered by the Death of an Extremely Massive Star like η Carinae, AJ **666**, 1116–1128 (2007).

[34] P. Ochner *et al.*, Asiago spectroscopic classification of MASTER OT J044212.20+230616.7 in PGC 1681539, The Astronomers Telegram **505**, 4890–4905 (201).

[35] H. Lin *et al.*, SN 2015bf: A fast declining type II supernova with flash-ionized signatures, MNRAS **505**, 4890–4905 (2021).

[36] C. L. Ransome *et al.*, A systematic reclassification of Type IIn supernovae, MNRAS **506**, 4715–4734 (2021)

[37] A. G. Riess, *et al.*, A Comprehensive Measurement of the Local Value of the Hubble Constant with 1 km s^{-1} Mpc^{-1} Uncertainty from the *Hubble Space Telescope* and the SH0ES Team, ApJ **934**, L7 (2022).

[38] Gaustad, J. E. *et al.* A Robotic Wide-Angle Hα Survey of the Southern Sky, PASP **113**, 1326-1348 (2001).

[39] C. G. Hoopes, R. A. M. Walterbos, The Contribution of Field OB Stars of the Diffused Ionized Gas in M33, ApJ **541**, 597-609 (2000).

[40] P. A. Crowther, Physical Properties of Wolf-Rayet Stars, Annual Review of Astronomy & Astrophysics **45**, 177-219.

A Python code for NCR values of images

```
import numpy as np
import astropy.io
import pandas as pd
from astropy.io import fits

hdu1=astropy.io.fits.open('m33_12_bin_noise.fits')
data=hdu1[0].data
y = len(data[0])
x = len(data)
amount = x*y
sum = 0
datagrid=np.ndarray(shape=(x,y),dtype=float,order='F')
for i in range(x-1):
    for j in range(y-1):
        datagrid[i,j]=data[i,j]


for i in range(x-1):
   for j in range(y-1):
      sum = sum + datagrid[i,j]
totalsum = sum



xx = []
yy =[]
for i in range(x):
    for j in range(y):
         xx.append(i)
         yy.append(j)



flatteneddatagrid = datagrid.flatten()
dataframe = pd.DataFrame()
dataframe['value'] = flatteneddatagrid
dataframe['x'] = xx
dataframe['y'] = yy




sorteddataframe = dataframe.sort_values(by=['value'])
sorted = sorteddataframe['value'].to_numpy()


pixelsum = 0
NCRn = []
for i in sorted:
        pixelsum = pixelsum + i
        if (pixelsum / totalsum) < 0:
             NCRn.append(0)
```

```
        else:
             NCRn.append(pixelsum / totalsum)



sorteddataframe['NCR'] = NCRn

imagedataframe = sorteddataframe.sort_index()

print(imagedataframe)
imagedataframe.to_csv('NCR_12_m33.csv', index=False)
```

B Python code for NCR values of stars

```
import numpy as np
import astropy.io
import pandas as pd
import matplotlib
import random
import statistics
from astropy.io import fits
from astropy.wcs import WCS
from matplotlib import pyplot as plt
from astropy.utils.data import get_pkg_data_filename
from astropy import units as u
from astropy.coordinates import SkyCoord
from itertools import cycle, islice, repeat

list = open('lmc_ysg_lum4_8+.txt', 'r')
listnew = []

for element in list:
        c = SkyCoord(element, unit = (u.hourangle,u.deg))
        listnew.append(c)

table = []
NCRtable = []
extendedlist = []
for i in range(0,100):
        extendedlist.extend(listnew)
print(len(extendedlist))

for i in extendedlist:
        x = random.randint(1, 76)
        if x in range(1, 7):
                image = 'lmc_79_bin_noise.fits'
                NCRfile = 'NCR_79_lmc.csv'
        if x in range(7, 13):
                image = 'lmc_74_bin_noise.fits'
                NCRfile = 'NCR_74_lmc.csv'
        if x in range(13, 21):
                image = 'lmc_71_bin_noise.fits'
```

```
            NCRfile = 'NCR_71_lmc.csv'
    if x in range(21, 27):
            image = 'lmc_67_bin_noise.fits'
            NCRfile = 'NCR_67_lmc.csv'
    if x in range(27, 35):
            image = 'lmc_62_bin_noise.fits'
            NCRfile = 'NCR_62_lmc.csv'
    if x in range(35, 41):
            image = 'lmc_59_bin_noise.fits'
            NCRfile = 'NCR_59_lmc.csv'
    if x in range(41, 46):
            image = 'lmc_56_bin_noise.fits'
            NCRfile = 'NCR_56_lmc.csv'
    if x in range(46, 51):
            image = 'lmc_49_bin_noise.fits'
            NCRfile = 'NCR_49_lmc.csv'
    if x in range(51, 55):
            image = 'lmc_42_bin_noise.fits'
            NCRfile = 'NCR_42_lmc.csv'
    if x in range(55, 62):
            image = 'lmc_35_bin_noise.fits'
            NCRfile = 'NCR_35_lmc.csv'
    if x in range(62, 65):
            image = 'lmc_30_bin_noise.fits'
            NCRfile = 'NCR_30_lmc.csv'
    if x in range(65, 69):
            image = 'lmc_26_bin_noise.fits'
            NCRfile = 'NCR_26_lmc.csv'
    if x in range(69, 73):
            image = 'lmc_16_bin_noise.fits'
            NCRfile = 'NCR_16_lmc.csv'
    if x in range(73, 75):
            image = 'lmc_12_bin_noise.fits'
            NCRfile = 'NCR_12_lmc.csv'
    if x in range(75, 77):
            image = 'lmc_7_noise.fits'
            NCRfile = 'NCR_7_lmc.csv'

    f = fits.open(image)
    w = WCS(f[0].header)
    x, y = w.world_to_pixel(i)

    X = x + np.random.normal(0.0, 1)
    Y = y + np.random.normal(0.0, 1)

    Y = round(Y)
    X = round(X)

    table.append([X, Y])

    tabledataframe = pd.DataFrame(table, columns=['Xvalue', '
                                        Yvalue'])
    NCRfileDF = pd.read_csv(NCRfile)
```

```
        x = (NCRfileDF.loc[(NCRfileDF['x'] == Y) & (NCRfileDF['y']
                                                == X)])
        if x.empty:
                NCRtable.append(0)
        else:
                x.to_numpy().flatten()
                NCRtable.append(x['NCR'].to_numpy())

NCRtablemean = np.average(NCRtable)
print('meanvalue=', NCRtablemean)

NCRtablestd = np.std(NCRtable)
print('standarddeviation=', NCRtablestd)

np.savetxt('lmc_ysg_lum4_8+_100x.txt', NCRtable)
```

C Python code for AD and KS tests

```
import numpy as np
import astropy.io
import pandas as pd
import matplotlib.pyplot as plt
import random
import statistics
from astropy.io import fits
from astropy.wcs import WCS
from matplotlib import pyplot as plt
from astropy.utils.data import get_pkg_data_filename
from astropy import units as u
from astropy.coordinates import SkyCoord
from itertools import cycle, islice
from scipy import stats
from scipy.stats import anderson_ksamp
from statistics import mean
from math import ceil, floor, sqrt

df = pd.read_csv('lmc_ysg_lum4_8+_ncr.txt')

NCRsorted = df.sort_values(by=['NCR'])

NCRsplit = NCRsorted[0::1]
meanvalue1list = []

for i in range(0, NCRsplit.size, 100):
        meanvalue1 = (NCRsplit['NCR'].iloc[i:i+100]).mean()


df2 = pd.read_csv('sn_ncr.txt')
NCRsorted2 = df2.sort_values(by=['NCR'])


NCRsplit2 = NCRsorted2[0::1]
```

```
meanvaluelist2 = []

for i in range(0, NCRsplit2.size, 1):
        meanvalue2 = (NCRsplit2['NCR'].iloc[i:i+1]).mean()

        meanvaluelist2.append(meanvalue2)


res = stats.anderson_ksamp([meanvalue1list, meanvaluelist2])

variable = np.array([res.significance_level])
np.savetxt('ad_lmc_ysg_lum4_8+.txt', variable)


ks = stats.ks_2samp(meanvalue1list, meanvaluelist2)
variable2 = np.array([ks.pvalue])
np.savetxt('ks_lmc_ysg_lum4_8+.txt', variable2)
```